High Pressure Beamline at NSLS and APS BM6

2014 COMPRES Annual Report

June 2014 – May 2015

Prepared by:

Donald J. Weidner

Lars Ehm

Tom Duffy

Michael T. Vaughan

Matthew Whitaker

Haiyan Chen

Xinguo Hong

Table of Contents

Part I: X17-DAC: Diamond Anvil Cell Facility at NSLS June, 2014 – September, 2014

I) Overview

The diamond anvil cell X-ray (X17-DAC) facility at the National Synchrotron Light Source (NSLS) is located on a superconducting wiggler beamline and consists of two dedicated high-pressure endstations (X17C and X17B3) and a sample preparation/spectroscopy laboratory. The superconducting wiggler source is a 5-pole device operated at 4.2 Tesla.

At X17C, angle and energy dispersive x-ray diffraction on polycrystalline samples is conducted in either axial or radial geometry. Energy dispersive single-crystal diffraction for phase identification, orientation determination, and unit cell refinement is also available (although not often requested anymore). X-rays are focused to 15 x 20 μm using a pair of Kirkpatrick-Baez mirrors. For angle dispersive experiments a Laue monochromater is used to provide 20-40 keV X-rays. Detectors in use are a Rayonix SX-165 (angle dispersive) and Canberra Ge solid state detector (energy dispersive).

X17B3 supports experiments at two x-ray energies: ~40 keV and ~80 keV. In the lower energy range, angle and energy dispersive diffraction experiments are carried out, similar to the capabilities at X17C. A double-sided laser heating system is available. At 80 keV, total scattering pair distribution function (PDF) measurements are performed. This technique involves measuring both Bragg and diffuse scattering for structural analysis of complex materials, allowing determination of local atomic structure for both crystalline and amorphous materials. Our detector at this beamline is a Perkin-Elmer flat panel detector (XRD 1621) which is optimized for high-energy radiation but also works effectively for experiments near 40 keV.

We have recently succeeded in focusing hard X-rays at 60 or 80 keV down to 15 x 15 μm using a pair of Kirkpatrick-Baez mirrors, and accommodated users to conduct PDF measurement using focused hard X-ray microbeam in the last two cycles of NSLS in 2014. PDF data on nano gold and silver have been obtained up 70 GPa. At X17B3 station, a double-side laser heating system for diamond anvil cell experiments has been designed and setup. The system uses a 100 W fiber laser. The compact system is built on a small 2’ x 3’ optical breadboard. The temperature measurement system is still under construction.

Our high-pressure sample preparation laboratory houses equipment for DAC sample preparation and includes a micro EDM (electric discharge machine) system, mechanical microdrill, high-resolution optical microscopes, electrical work station, mechanical work bench, sample loading tools, DAC tools, standard samples, pressure media and pressure indicators. A cryogenic gas loading system is available (nitrogen and argon) as well as the capability to obtain gas loading from the GSECARS/COMPRES system at APS via a mail-in service.

Our sample preparation lab and ruby spectroscopy system are used annually by more than 100 users from 9 or more beamlines (X17C, X17B3, U2A, X17B1, X17B2, X17A, X14A,

X27A, X3A). We have completely revamped this laboratory and all major equipment is now updated. We have a wide selection of diamond anvil cells available for beamline staff and users including symmetric and panoramic cells as well as an Almax-Boehler plate DAC.

Operation of the NSLS ceased on September 30, 2014, and this report covers activity through that date.

II) X17-DAC – User Community at a Glance

Total # of Proposals received

2010 – 73

2011 – 93

2012 – 96

2013 – 88

2014 – 56

Oversubscription: ~2.2

User Community (2011-2014)

Research groups: 57

Institutions: 33

(24 COMPRES members or foreign affiliates)

Unique Users: ~145

III) Scientific Highlights

A total of 34 publications have been recorded through October, 2014 and a total of 29 and 31 publications were recorded for 2013 and 2012, respectively. Our long-term trend is generally steady with ~30-40 publications per year. A total of 268 publications have been recorded since 2007.

Some scientific highlights for 2013-2014:

Highlight list:

1) Equation of state of a synthetic ulvöspinel, $(Fe_{1.94}Ti_{0.03})TiO_4$, at ambient temperature.
2) The role of carbon in extrasolar planetary geodynamics and habitability.
3) Equation of state of pyrope–almandine solid solution measured using a diamond anvil cell and in situ synchrotron X-ray diffraction.
4) X-ray absorption spectroscopy of GeO_2 glass to 64 GPa.
5) Polyhedral units and network connectivity in GeO_2 glass at high pressure: An X-ray total scattering investigation.
6) Bulk Signatures of Pressure-Induced Band Inversion and Topological Phase Transitions in $Pb_{1-x}Sn_xSe$.
7) Swift heavy ion-induced phase transformation in Gd_2O_3.
8) Structural phase transition of $BaZrO_3$ under high pressure.
9) Pressure-induced phase transitions in rubidium azide: Studied by in-situ x-ray diffraction.

Work at NSLS Highlighted In Other Publications

1) **Journal of Physics Condensed Matter Labtalk Highlight**: X-ray absorption spectroscopy probes germanium dioxide glass.
2) **Photon Sciences eNews highlight:** Pressure transforms a semiconductor into a new state of matter.

1) Equation of state of a synthetic ulvöspinel, $(Fe_{1.94}Ti_{0.03})TiO_4$, at ambient temperature

Using a diamond-anvil cell and synchrotron X-ray diffraction, the compressional behavior of a synthetic ulvöspinel $(Fe_{1.94}Ti_{0.03})TiO_4$ has been investigated up to about 7.05 GPa at 300 K. The pressure–volume data fitted to the second-order Birch–Murnaghan equation of state yield an isothermal bulk modulus (K_T) of 147(4) GPa (K'_T fixed as 4). This value is slightly larger than that previously determined by an ultrasonic pulse echo method (121(2) GPa; Syono et al., *J Phys Soc Jpn* **31**:471–476, 1971), but substantially smaller than that recently determined by a synchrotron X-ray diffraction technique (251(3) GPa; Yamanaka et al., *Phys Rev B* **80**:134120, 2009; *Am Mineral* **98**:736–744, 2013). Combined with the K_T of magnetite (Fe_3O_4; ~182(3) GPa), our finding suggests that the bulk modulus of the solid solutions $Fe_{3-x}Ti_xO_4$ $(0 \le x \le 1)$ along the join magnetite–ulvöspinel decreases by ~20 %.

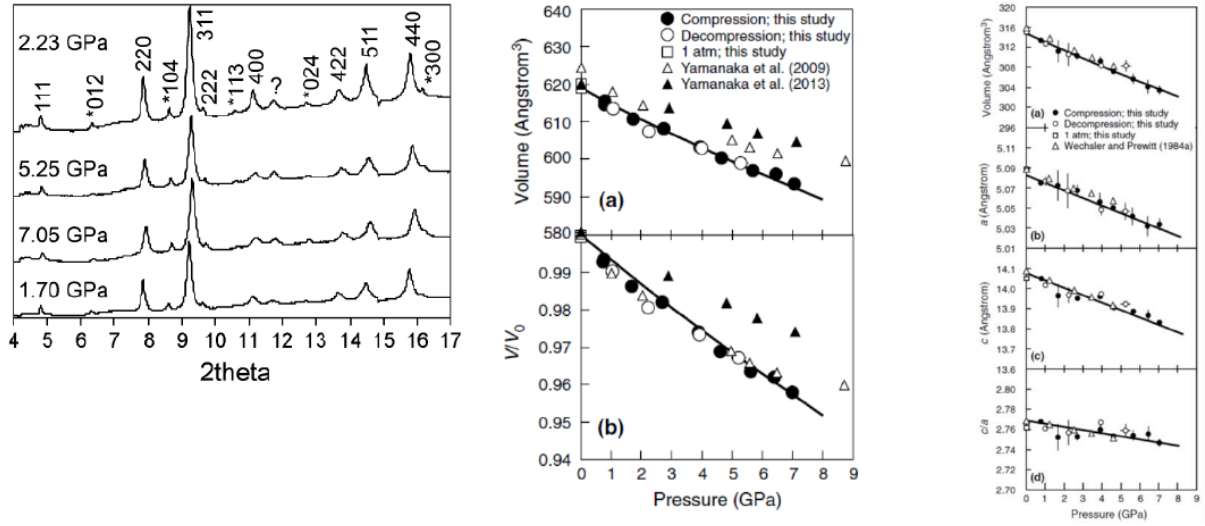

Figure 1. Left panel: Examples of X-ray diffraction patterns of ulvöspinel at 1.70, 7.05, 5.25 and 2.23 GPa. Middle panel: Effect of pressure on the unit-cell parameters of ulvöspinel at 300 K, compared to those from Yamanaka et al. (2009, 2013): **a** the volume; **b** the $V/V0$ ratio. Right panel: Effect of pressure on the unit-cell parameters of ilmenite at 300 K, compared to those from Wechsler and Prewitt (1984). *Thick curve* represents the second-order Birch–Murnaghan equation of state, established using all P–V data collected in this study.

Reference: Xiong Z, Liu X, Shieh S R, Wang F, Wu X, Hong X and Shi Y (2014) Equation of state of a synthetic ulvöspinel, $(Fe_{1.94}Ti_{0.03})TiO_4$, at ambient temperature *Phys Chem Minerals* **41**, 1–7

2) The role of carbon in extrasolar planetary geodynamics and habitability

The proportions of oxygen, carbon, and major rock-forming elements (e.g., Mg, Fe, Si) determine a planet's dominant mineralogy. Variation in a planet's mineralogy subsequently affects planetary mantle dynamics as well as any deep water or carbon cycle. Through thermodynamic models and high pressure diamond anvil cell experiments, we demonstrate that the oxidation potential of C is above that of Fe at all pressures and temperatures, indicative of 0.1-2 Earth-mass planets. This means that for a planet with (Mg+2Si+Fe+2C)/O > 1, excess C in the mantle will be in the form of diamond. We find that an increase in C, and thus diamond, concentration slows convection relative to a silicate-dominated planet, due to diamond's ~3 order of magnitude increase in both viscosity and thermal conductivity. We assert then that in the C-(Mg+2Si+Fe)-O system, there is a compositional range in which a planet can be habitable. Planets outside of this range will be dynamically sluggish or stagnant, thus having limited carbon or water cycles leading to surface conditions inhospitable to life as we know it.

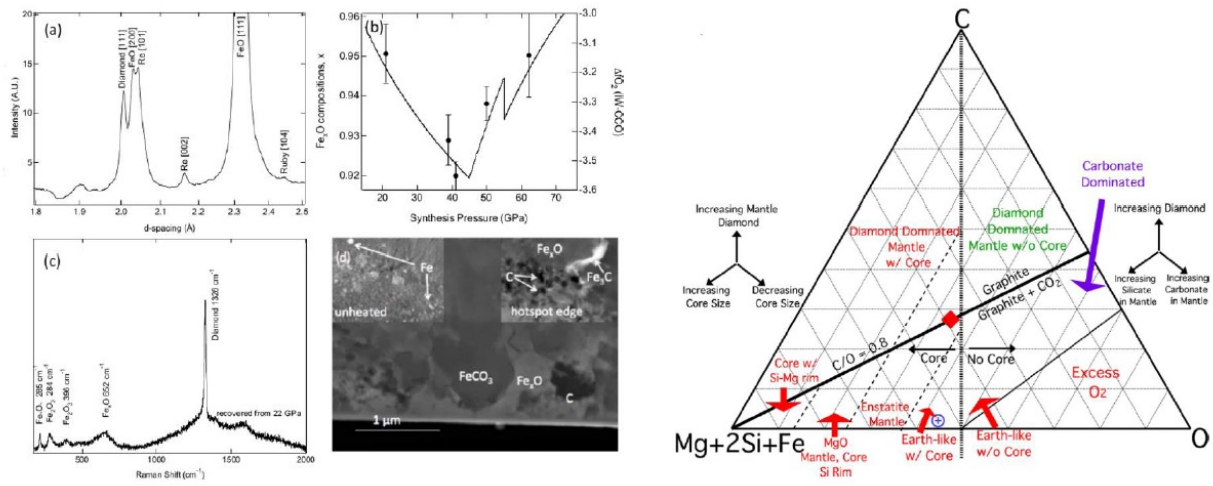

Figure 2. Left panel: Reactions between FeO, $FeCO_3$, and Fe at 21–63 GPa and 2150(150) K show the oxidation of iron and reduction of carbon. (a) X-ray diffraction at 43 GPa shows the presence of diamond and wüstite with no evident siderite. (b) The unit cell volume of the recovered sample. (c) Raman spectroscopy of a sample recovered from 22 GPa. (d) TEM image of a foil extracted by focused-ion beam milling from a sample recovered from 63 GPa and 2200 K. Right panel: Ternary diagram for the C–(Mg+2Si+Fe)–O system..

Reference: Unterborn, C, J Kabbes, J Pigott, D Reaman and W Panero. (2014) The Role of Carbon in Extrasolar Planetary Geodynamics and Habitability, *The Astrophysical Journal* **793** (2): 124.

3) Equation of state of pyrope–almandine solid solution measured using a diamond anvil cell and in situ synchrotron X-ray diffraction

The pressure–volume relations of three synthetic garnet samples, $Py_{83}Alm_{17}$, $Py_{54}Alm_{46}$ and $Py_{30}Alm_{70}$,along pyrope–almandine (Py–Alm) join were measured at ambient temperature and high pressures up to 7, 21 and 19 GPa, respectively. The obtained *P–V* data were fitted to the third-order Birch–Murnaghan equation of state (EOS). The ambient cell volumes V_0 of the three samples were measured to be 1511(1), 1515(2), and 1526(1) $Å^3$ respectively. With fixed pressure derivative of the isothermal bulk modulus, K', at 4.3, isothermal bulk moduli, $K_{0,}$ of the three samples were determined to be 172(4), 174(2), and 183(2) GPa respectively. These results confirm that almandine content (iron substitution) increases the bulk modulus of the garnet join following a nearly ideal mixing model. The relation between bulk modulus and almandine mole fraction (n) in this garnet join is derived to be $K_0 = 170 + 15\ n$. These data can be used to contribute to construction of compositional models of Earth's mantle.

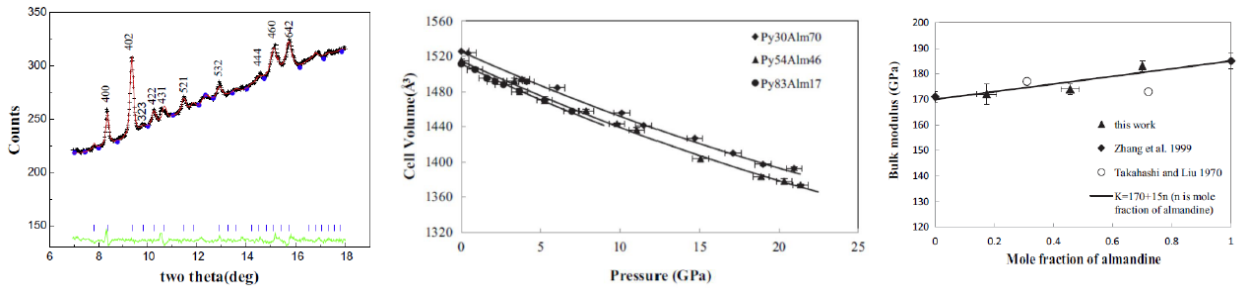

Figure 3. Left panel: Le Bail fitting of $Py_{30}Alm_{70}$ at 19 GPa and room temperature. Middle panel: Volume of Py–Alm garnets as a function of pressure measured using in situ X-ray diffraction at room temperature. Uncertainties of volume data are smaller than symbols. Solid lines represent the third order Birch–Murnagahan EOS fitting. Right panel: Bulk modulus data of almandine–pyrope binary system.

Reference: Huang S and Chen J (2014) Equation of state of pyrope-almandine solid solution measured using a diamond anvil cell and in situ synchrotron X-ray diffraction *Physics of the Earth and Planetary Interiors*, **228**: 88-91.

4) X-ray absorption spectroscopy of GeO_2 glass to 64 GPa

The structural behavior of GeO_2 glass has been investigated up to 64 GPa using results from x-ray absorption spectroscopy in a diamond anvil cell combined with previously reported density measurements. The difference between the nearest Ge–O distances of glassy and rutile-type GeO_2 disappears at the Ge–O distance maximum at 20 GPa, indicating completion of the tetrahedral–octahedral transition in GeO_2 glass. The mean-square displacement σ^2 of the Ge–O distance in the first Ge–O shell increases progressively to a maximum at 10 GPa, followed by a substantial reduction at higher pressures. The octahedral glass is, as expected, less dense and has a higher compressibility than the corresponding crystalline phase, but the differences in Ge–O distance and density between the glass and the crystals are gradually eliminated over the 20–40 GPa pressure range. Above 40 GPa, GeO_2 forms a dense octahedral glass with a compressibility similar to that of the corresponding crystalline phase (α-PbO_2 type). The EXAFS and XANES spectra show evidence for subtle changes in the dense glass continuing to occur at these high pressures. The Ge–O bond distance shows little change between 45–64 GPa, and this may reflect a balance between bond shortening and a gradual coordination number increase with compression. The density of the glass is similar to that of the α–PbO_2-type phase, but the Ge–O distance is longer and is close to that in the higher-coordination pyrite-type phase which is stable above ~60 GPa. The density data provide evidence for a possible discontinuity and change in compressibility at 40–45 GPa, but there are no major changes in the corresponding EXAFS spectra. A pyrite-type local structural model for the glass can provide a reasonable fitting to the XAFS spectra at 64 GPa.

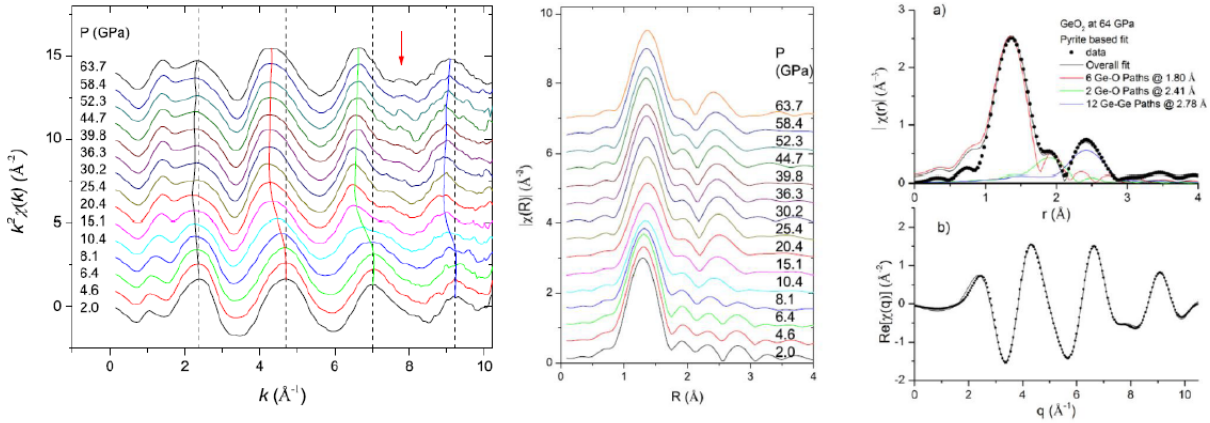

Figure 4. Left panel: k^2-weighted XAFS spectra, $k^2\chi(k)$, for GeO_2 glass at high pressures. Middle panel: XAFS Fourier transform, $|\chi(R)|$, for GeO_2 glass at high pressures. Note the merging of two peaks (2.2—3Å) at 10.4 GPa. Right panel: The pyrite-based structural modelling for GeO_2 glass at 63.7 GPa (full circles).

Reference: Hong X, Newville M, Duffy T, Sutton S and Rivers M, "X-Ray Absorption Spectroscopy of GeO_2 Glass to 64 GPa." *Journal of Physics: Condensed Matter* 26, no. 3 (2014): 035104.

5) Polyhedral units and network connectivity in GeO_2 glass at high pressure: An X-ray total scattering investigation

The authors report a pressure-induced dense tetrahedral intermediate state via Ge–O–Ge rotation formed at 3–5 GPa and the polyhedral relations in GeO_2 glass up to 17.5 GPa using *in situ* X-ray total scattering and X-ray absorption (XAFS) techniques. It was found that the nearest-neighbor Ge–Ge correlations show a decrease reaching a minimum between 4 and 6 GPa, and exhibit negative compression behavior at 7–17.5 GPa. The Ge–Ge distance determined by XAFS shows a substantial reduction, i.e., normal compression behavior, at 7–17.5 GPa. The comparison with the theoretical *g(r)* function for rutile-type GeO_2 (16.1GPa) indicates that the negative compression of intermediate range order reflects the direct formation of GeO_6 octahedral units. Results of coordination number analysis show that GeO_2 glass undergoes a transition from tetrahedral GeO_4, to GeO_5 units (possibly triangular bipyramidal), and finally to octahedral GeO_6 units. The present investigation provides the structural details of the polyhedral units and their relationships in GeO_2 glass at high pressure.

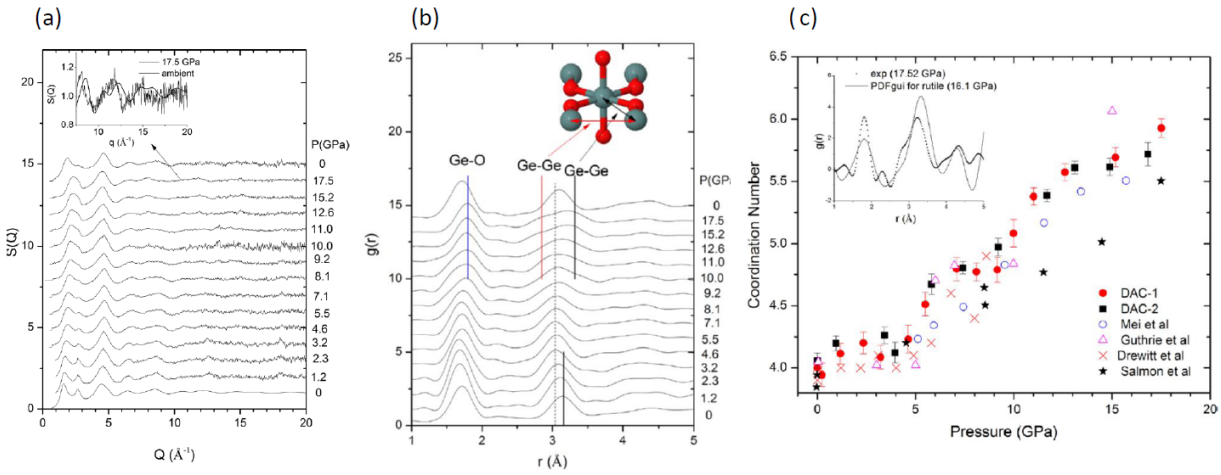

Figure. 5. (a) Structure factor, *S(Q)*, for GeO_2 glass at different pressures; (b) Pair distribution function *g(r)* for GeO_2 glass; (c) The pressure evolution of the mean coordination number N_{Ge}^{O} for GeO_2 glass

Reference: Hong X, Ehm L and Duffy T S 2014 Polyhedral units and network connectivity in GeO2 glass at high pressure: An X-ray total scattering investigation *Applied Physics Letters* **105** 081904

6) Bulk Signatures of Pressure-Induced Band Inversion and Topological Phase Transitions in $Pb_{1-x}Sn_xSe$

The characteristics of topological insulators are manifested in both their surface and bulk properties, but the latter remain to be explored. In this paper, the authors report bulk signatures of pressure-induced band inversion and topological phase transitions in $Pb_{1-x}Sn_xSe$ (x = 0.00, 0.15, and 0.23). The results of infrared measurements as a function of pressure indicate the closing and the reopening of the band gap as well as a maximum in the free carrier spectral weight. The enhanced density of states near the band gap in the topological phase gives rise to a steep inter-band absorption edge. The change of density of states also yields a maximum in the pressure dependence of the Fermi level. Thus, the conclusive results

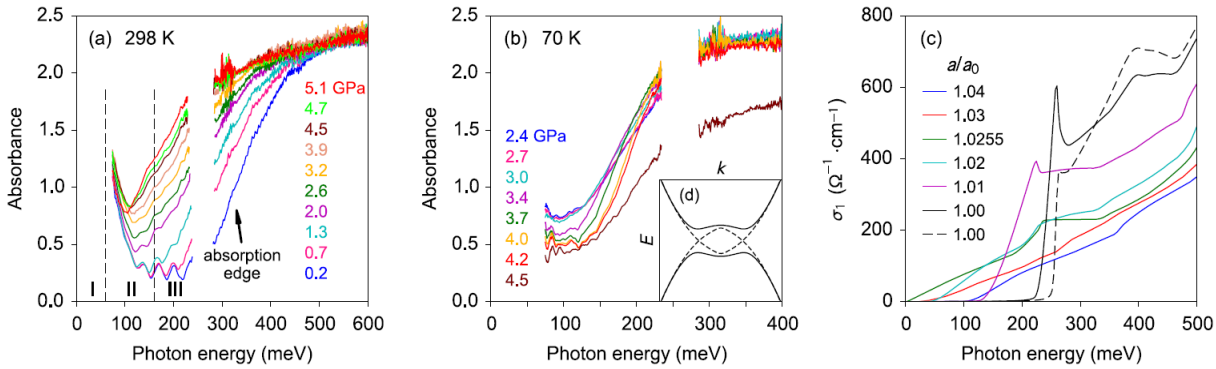

provide a consistent picture of pressure-induced topological phase transitions and highlight the bulk origin of the novel properties in topological insulators.

Figure. 6. Pressure-dependent mid-infrared absorbance of PbSe measured at (a) 298 K and (b) 70 K. Data in the blank region between 200–300 meV are not shown because of unreliability caused by diamond absorption. (c) Real part of the interband optical conductivity σ1 of intrinsic PbSe at various $a=a_0$ from first-principles calculations. The dashed line shows the result including holes with a density of 1018 cm^{-3}. (d) [inset to (b)] A diagram illustrating hybridization opens up a band gap (in the bands shown as solid lines) when the conduction band and valence band cross (dashed lines).

Reference: Xi X, He X-G, Guan F, Liu Z, Zhong R D, Schneeloch J A, Liu T S, Gu G D, Xu D, Chen Z, Hong X G, Ku W and Carr G L 2014 Bulk Signatures of Pressure-Induced Band Inversion and Topological Phase Transitions in $Pb_{1-x}Sn_xSe$ *Phys. Rev. Lett.* **113** 096401

7) Swift heavy ion-induced phase transformation in Gd_2O_3

The authors report that the crystalline-to-crystalline phase transformation of cubic Gd_2O_3 induced by swift Au ions with a kinetic energy of 2.25 GeV, has been characterized by synchrotron X-ray diffraction experiments (XRD) as a function of increasing fluence, up to 5×10^{13} ions/cm^2. The diffraction maxima of the initial cubic structure gradually decrease in intensity as function of ion fluence, concurrent with the in-growth of several new diffraction peaks, which, based on Rietveld refinement, correspond to the monoclinic high-temperature phase. The same cubic-to-monoclinic phase transformation induced by swift heavy ions has been observed in Y_2O_3. The transformation pathway under irradiation is consistent with the high-temperature behavior of Gd_2O_3, and is probably associated with a multiple ion-impact mechanism. There was no evidence of amorphous material in the diffraction patterns, even after irradiation to the maximum fluence, at which the initial cubic phase has been completely transformed to the monoclinic structure.

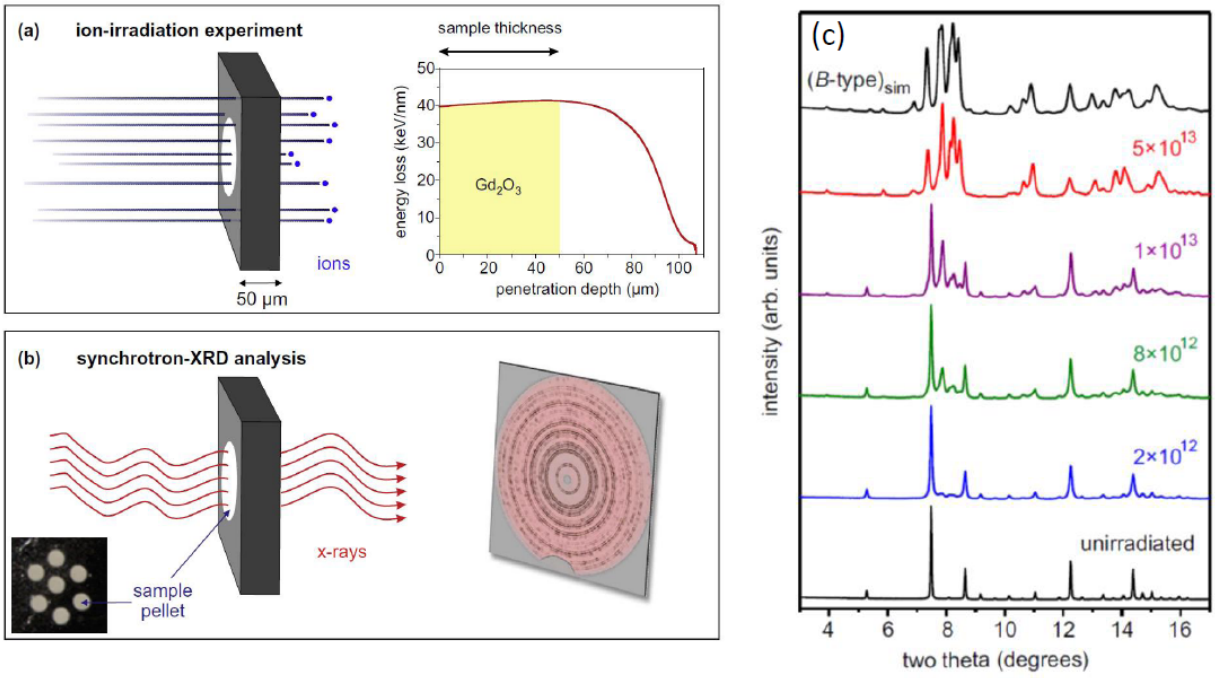

Figure 7. (a) Swift Au ions of 2.25 GeV kinetic energy completely penetrate the (white) powder sample pressed into a thin steel foil; (b) Powder X-ray diffraction experiments with 30.5 keV X-rays to study ion-induced structural modifications throughout the sample thickness; (c) Synchrotron X-ray diffraction patterns of Gd2O3 before and after irradiation with 2.25 GeV Au ions.

Reference: Lang M, Zhang F, Zhang J, Tracy C L, Cusick A B, VonEhr J, Chen Z, Trautmann C and Ewing R C 2014 Swift heavy ion-induced phase transformation in Gd_2O_3 *Nuclear Instruments and Methods in Physics Research Section B: Beam Interactions with Materials and Atoms* **326** 121–5

8) Structural phase transition of $BaZrO_3$ under high pressure

The authors report the phase transition behavior of cubic $BaZrO_3$ perovskite by *in situ* high-pressure synchrotron X-ray diffraction experiments up to 46.4 GPa at room temperature. The phase transition from the cubic phase to the tetragonal phase was observed in $BaZrO_3$ for the first time, which takes place at 17.2 GPa. A bulk modulus 189(26) GPa for cubic $BaZrO_3$ is derived from the pressure–volume data. Upon decompression, the high-pressure phase transforms into the initial cubic phase. It is suggested that unstable phonon modes caused by the rotation of oxygen octahedra plays a crucial role in the high-pressure phase transition behavior of $BaZrO_3$.

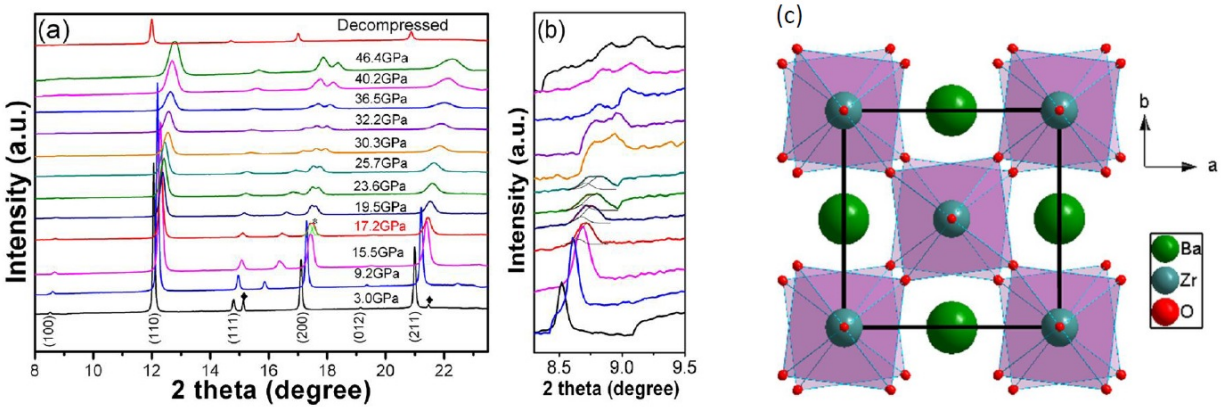

Figure 8. (a) Selected XRD patterns of $BaZrO_3$ as a function of pressure upon compression up to 46.4 GPa; (b) The enlarged pattern in the region of 8–9.5 of $BaZrO_3$. The asterisk denotes the new peak. The peaks marked by the diamond denote the unknown peaks; (c) Schematic representation of $BaZrO_3$ in I4/mcm space group structure with oxygen octahedra rotation. View along the c direction, where the out-of-phase tilting of oxygen octahedra occurs.

Reference: Yang X, Li Q, Liu R, Liu B, Zhang H, Jiang S, Liu J, Zou B, Cui T and Liu B 2014 Structural Phase Transition of $BaZrO_3$ under High Pressure *Journal of Applied Physics* **115 (** 12): 124907:1-5

9) Pressure-induced phase transitions in rubidium azide: Studied by in-situ x-ray diffraction

The authors present the in-situ X-ray diffraction studies of RbN_3 up to 42 GPa at room temperature to supplement the high-pressure exploration of alkali azides. Two pressure-induced phase transitions of α-RbN_3 → γ-RbN_3 → δ-RbN_3 were revealed at 6.5 and 16.0 GPa, respectively. During the phase transition of α-RbN_3 → γ-RbN_3, lattice symmetry decreases from a fourfold to a twofold axis accompanied by a rearrangement of azide anions. The γ-RbN_3 was identified to be a monoclinic structure with *C2/m* space group. Upon further compression, an orthogonal arrangement of azide anions becomes energetically favorable for δ-RbN_3. The compressibility of α-RbN_3 is anisotropic due to the orientation of azide anions. The bulk modulus of α-RbN_3 is 18.4 GPa, quite close to those of KN_3 and CsN_3. By comparing the phase transition pressures of alkali azides, their ionic character is found to play a key role in pressure-induced phase transitions.

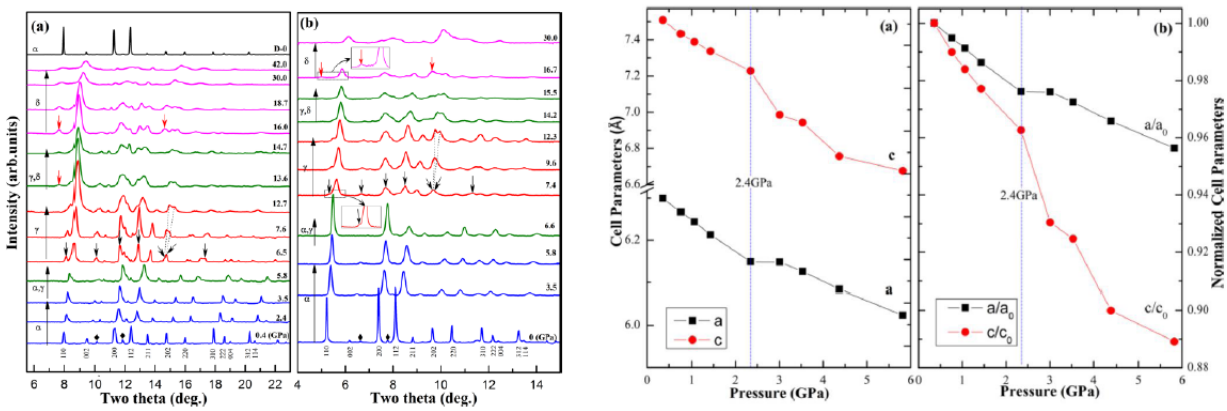

Figure 9. Left panel: Representative the XRD patterns of RbN_3 at various pressures. Wavelengths of X-ray used in (a) 0.6199 Å and (b) 0.4066 Å. The arrows (↓) denote the new peaks of high pressure phases. The diamonds (◆) denote the peaks of the unidentified impurity, and dashed lines serve as visual guides for these two neighboring peaks. Insets in (b): blowup of the Bragg peaks in orthogons. Right panel: Pressure dependence of the cell parameters. (b) Compression ratio (a/a_0, c/c_0) of α-RbN_3.

Reference: Li D, Wu X, Jiang J, Wang X, Zhang J, Cui Q and Zhu H 2014 Pressure-induced phase transitions in rubidium azide studied by in-situ x-ray diffraction Applied Physics Letters 105 071903

Work at NSLS Highlighted In Other Publications

1) Journal of Physics Condensed Matter Labtalk Highlight:

X-ray absorption spectroscopy probes germanium dioxide glass

SiO_2 and GeO_2 glasses are prototypical strong network-forming glasses, which have been extensively investigated because of their importance in condensed matter physics, materials science and geology. The high-pressure behaviour of SiO_2 glass is of geological interest as a model system for silicate melts in the Earth's interior. Germania, GeO_2, is regarded as a good chemical and structural analogue of silica (SiO_2), but, unlike silica, the local structure of the Ge atoms can be studied effectively by the x-ray absorption fine structure (XAFS) techniques in a diamond anvil cell (DAC). In *J. Phys.: Condens. Matter* **26** 035104, we present high pressure XAFS and density studies of GeO_2 glass.

XAFS is a powerful tool to determine the local and higher-order structure around absorber atoms in a material. A major problem with using conventional energy-scanning XAFS techniques in the diamond cell environment are the glitches imposed on the spectrum due to single-crystal x-ray reflections from the diamond anvils. Here we use a recently developed iterative method to effectively remove these glitches and obtain high-quality XAFS data with the energy-scanning technique. We combine our new XAFS data with previously reported density measurements on GeO_2 glass at high pressures to show that germania undergoes a continual structural evolution under high pressure to 64 GPa.

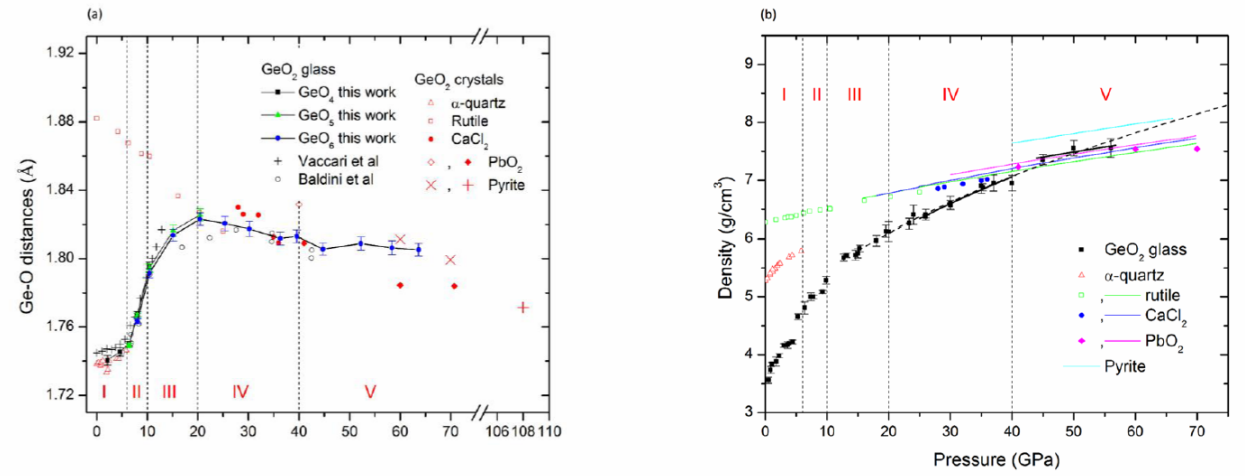

Figure 10. (a) Evolution of the nearest Ge–O distance of GeO_2 as a function of pressure. (b) Density of GeO_2 glass at high pressure. Dashed lines mark the five distinct regions characterizing the pressure response of GeO_2 glass.

The compression behaviour of GeO_2 glass can be divided into five distinct regions. Below 6 GPa (region 1), the distance between the germanium and oxygen atoms (Ge–O) is consistent with that of α-quartz GeO_2 and the density increases greatly with pressure (figure 1(a)). As pressure increases, the difference between the nearest Ge–O distances of glassy and rutile-type GeO_2 disappears at the Ge–O distance maximum at 20 GPa, indicating completion of the tetrahedral–octahedral transition in GeO_2 glass (regions II and III).

At 20–40 GPa, there is a continuous decrease in the Ge–O bond distance. The octahedral glass is less dense and has a higher compressibility than the crystalline phases that are stable at these pressures (figure 1(b), region IV). Above 45 GPa, the density and compressibility of the glass become very similar to those of the corresponding crystalline phases (region V). In this range, the Ge–O bond distance remains nearly constant with pressure, which may reflect a balance between bond shortening under compression and bond lengthening due to a gradual coordination number increase. The pyrite-type structure is the stable polymorph of GeO_2 glass above ~ 60 GPa and a pyrite-type local structural model with 6+2 coordination for the glass can provide a reasonable fitting to the XAFS spectra at 64 GPa.

Reference: http://iopscience.iop.org/0953-8984/labtalk-article/55720.

2) NSLS e-news: Pressure transforms a semiconductor into a new state of matter

By applying pressure to a semiconductor, researchers have been able to transform a semiconductor into a "topological insulator" (TI), an intriguing state of matter in which a material's interior is insulating but its surfaces or edges are conducting with unique electrical properties. This is the first time that researchers have used pressure to gradually "tune" a material into the TI state; as such, the study gives scientists a new route for discovery as they search for TIs that could be used in advanced electronics applications.

The group reports their results in the October 8 online edition of Physical Review Letters. The experiment was performed at Brookhaven National Laboratory's National Synchrotron Light Source (NSLS), with the transition into the TI state confirmed using beams of x-rays and infrared light.

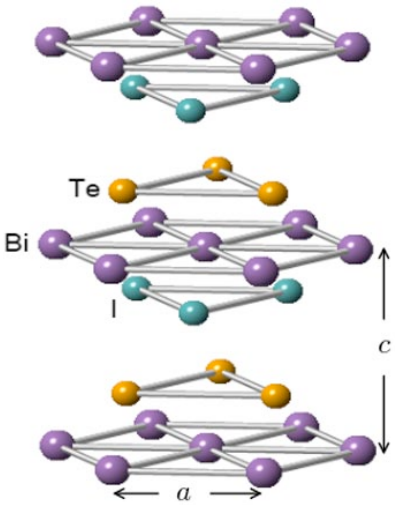

Figure 11. Crystal structure of bismuth-tellurium-iodine (BiTeI) semiconductor, with unit cell lengths labeled *a* and *c*

"Despite the well-known underlying physics of topological insulators, expanding the topological material family remains a challenge," said Brookhaven Lab Research Associate Xiaoxiang Xi, the paper's lead author. "Our experiment indicates that pressure is an effective

way to induce the topological insulating phase, and also that these techniques are useful for investigating the phase transitions that transform ordinary insulators into TIs."

In a TI material, the bulk interior cannot conduct, but the surfaces or edges, referred to as boundaries, contain electrons that are "locked" into a special arrangement of their spins (spin is the property of an electron that gives rise to magnetism). This spin structure is a result of the symmetry-protected metallic state in which electrons flow freely with little scattering and virtually no mass.

The semiconductor used in this study is a compound of bismuth, tellurium, and iodine (BiTeI). In similar compounds, researchers have induced the TI state either by doping (adding a small amount of an extra element) or by growing a sample on a substrate selected to introduce structural strain – and therefore slight structural changes – in the sample during the growth process. Both of these methods produce the necessary changes in electronic behavior that allow a material to behave as a TI. Both methods lead to other problems, however. Doping tends to induce defects and inhomogeneities in the sample, while the substrate-induced strain method does not allow researchers to continuously tune and controllably study the material and process that transforms an ordinary insulator into a TI.

Using pressure avoids these drawbacks. At NSLS, the researchers applied pressure to a BiTeI sample up to about 10 GPa, which is roughly equal to 100,000 times atmospheric pressure. They tracked the structural and electronic changes in the material using two synchrotron techniques, x-ray powder diffraction and infrared spectroscopy, performed at NSLS beamlines X17C and U2A, respectively. The analysis revealed that BiTeI transitions into a TI in the pressure range from 2 to 8 GPa.

The x-ray diffraction patterns show that the BiTeI crystal unit cell, the basic building block of the crystal (with lengths that are commonly denoted a, b, and c), undergoes a small, but telling, change between 2 and 2.9 GPa: The ratio of two of the lengths of the unit cell, c/a, reaches a minimum value. This indicates a strengthening of the bonding along the c direction – an expected change during the transition in this material.

The infrared data also show a key feature over the same pressure range: a maximum in the "plasma frequency," a quantity intimately related to the electronic structure and transport properties of the material. This feature is also something that is expected during a pressure-induced transition to the TI phase. It indicates that the BiTeI semiconducting energy gap – which normally prevents electrons in the material from participating in conduction – does close up and reopen as the pressure is swept through the transition region.

"The infrared feature is expected to be universal in pressure-induced topological phase transitions," says Xi. "Thus, we expect that infrared spectroscopy will be useful for investigating other candidate pressure-induced TIs that have been proposed by theory."

Reference: http://www.bnl.gov/ps/eNews/news.php?a=24481

IV) Progress in high-energy X-ray diffraction

The total scattering pair distribution function (PDF) technique using high-energy X-rays, which allows access to the high-resolution diffraction data with a large coverage of scattering vector, e.g. $20Å^{-1}$—$40Å^{-1}$. This is an emerging structural analysis method in high-pressure research. With this technique, it is possible to simultaneously probe the local, intermediate and long-range structure in crystalline, amorphous or complex materials. Using high-energy X-rays of 80 keV at X17B3 beamline at the National Synchrotron Light Source (NSLS) at Brookhaven National Laboratory, high-resolution X-ray diffraction and PDF measurements have been carried out by users from multiple disciplines.

There are two limitations imposed by the diamond anvil cell technique for the PDF or high resolution X-ray diffraction at high pressure, i.e. the open angle of DAC and the size of the focused X-ray beam.

Focusing the high energy X-ray beam

Although by using a Princeton-manufactured short piston-cylinder cell, users can readily carry out high-pressure PDF experiment up to 30 GPa using an unfocused beam, micron-sized focused X-ray beam is in high demand for DAC experiments. Recently, we have successfully focused the 80 keV X-ray beam using multilayer mirrors and Pt-coated mirrors to 20 × 50 μm^2 and 15 × 15 μm^2, respectively. Figure 7 shows the beam size measurement using the Pt-coated mirrors. A comparison of the data collected with unfocused and focused beam at 80 keV is shown in figure 8. The refinement of the pair distribution function shown in figure 9 shows a benchmark of nanocrystalline silver at 50 GPa. While the spot size is smaller using the Pt-coated mirrors, the depth-graded multilayer mirrors may provide a higher intensity gain due to a larger acceptance angle. As extensively demonstrated at the X17B3 beamline, we will be able to provide the users with a variety of focusing options optimized for the needs of their experiments at the new XPD-D beamline at NSLS-II in the near future.

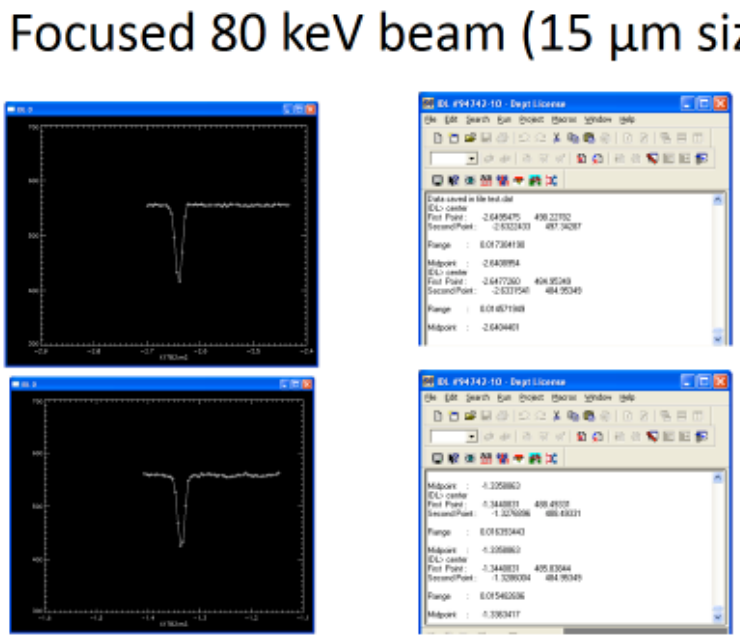

Figure 12. Successful focusing for hard 80 keV X-ray beam down to 15-micron size at X17B3 beamline.

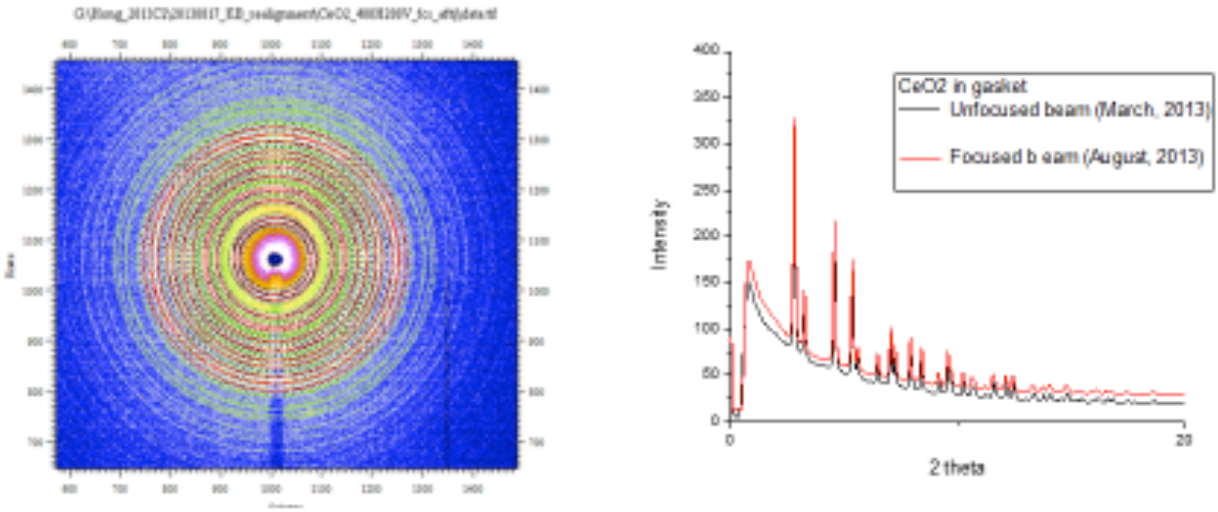

Figure 13. X-ray diffraction pattern of CeO_2 using focused 80 keV microbeam.

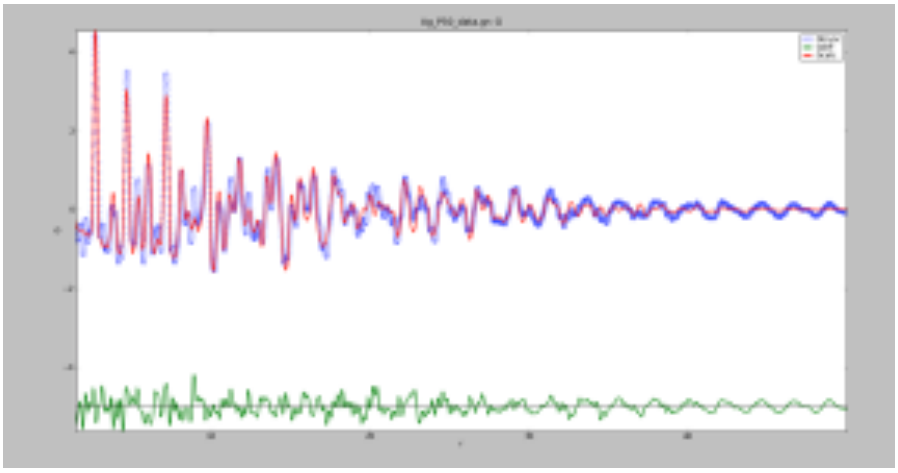

Figure 14. PDF fitting for nano-silver (20nm) at 50 GPa using 80 keV microbeam at X17B3 station.

Figure 10 shows the success of focusing the high-energy X-ray beam (66.099 keV and 81.088 keV) down to 15-μm size at X17B3 station, respectively. In combination with the recent developed large-opening cell, we can get the *Q*-coverage out 22 $Å^{-1}$.

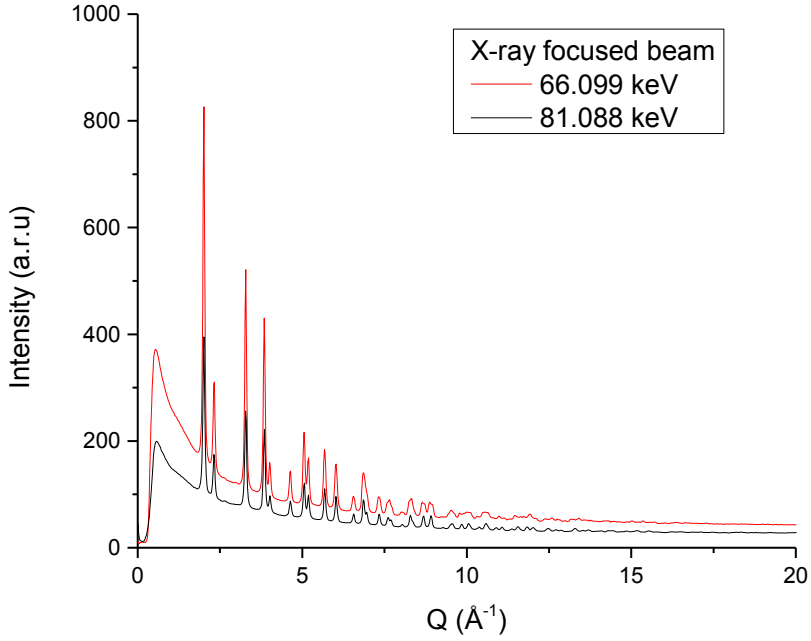

Figure 15. X-ray diffraction pattern of CeO_2 standard inside a DAC gasket at ambient using high-energy X-ray focused 66.099 keV and 81.088 keV beam at X17B3 station, respectively.

In summary, in combination with our developed method of precise X-ray energy calibration (Hong, Chen and Duffy, RSI 2012), which is indispensable for X-ray energy-sensitive scattering and diffraction experiments, we have offered the COMPRES community and other users the unique capability of HP-PDF experiments to study the structure of minerals under extreme conditions at X17B3 of NSLS. We intend to continue our development of HP-PDF at XPD-D at the National Synchrotron Light Source II. The X-ray Powder Diffraction beamline (XPD), the future home of the NSLS-II high-pressure program, provides high energy X-rays in the 30-70 keV range, which makes it ideally suited for HP-PDF experiments.

V) Beamline status and operations

Beamline Personnel

Since 2007, management team for X17-DAC is headed by PIs Donald Weidner (Stony Brook) and Thomas Duffy (Princeton). Our staff consisted of two beamline scientists: Xinguo Hong (since June 2010) and Zhiqiang Chen (Nov. 2008-Apr. 2014). Zhiqiang Chen was terminated at the end of April 2014 due to budget considerations. Xinguo Hong supported all users at the two endstations X17B3 and X17C during remaining NSLS operation.

Others who contribute to the effort include:

Lars Ehm (BNL/SBU) is a Research Associate Professor at the Mineral Physics Institute at Stony Brook University and the Photon Science Directorate at Brookhaven National Laboratory. He provides support to the high-pressure program at X17 at no cost to COMPRES. Lars is also leading the diamond anvil cell effort at XPD of NSLS-II.

Sanjit Ghose (BNL/NSLS-II) is a project scientist for the XPD beamline of NSLS-II. He informally collaborates with X17-DAC focusing specifically on the development of multi-layer mirrors for focusing high-energy radiation. These mirrors are designed to fit within the current bended design for KB mirrors. Previous projects that Sanjit contributed to include: the implementation of the PE flat-panel detector, design and installation of a new universal detector mount, and general assistance with computers, communications, and controls.

We obtained support from a number of Stony Brook Mineral Physics staff members including Michael Vaughan, William Huebsch, Kenneth Baldwin and Samantha Lin. Mark Rivers of CARS provide extensive informal support covering motor control and electronics. Zhong Zhong is the Photon Sciences Directorate staff member who provided assistance in beamline operations and monochromator set-up and operation.

Beamline Operations

The X17C beamline is a side station that runs 100% of the time, and the number of days per cycle has ranged from 53-85 over the last two years. The X17B3 beamline operates 33% of the time in dedicated mode with an additional 33% in shared mode when the X17B2 (multi-anvil) station is running. We are assigned between 18-28 days per cycle at X17B3 in dedicated mode.

The X17 beamlines are NSLS Facility Beamlines with a Contributing User (CU) agreement with COMPRES. The NSLS is responsible for the operation of the beamline (optics, safety systems, etc.) while COMPRES is responsible for operation of the experimental stations. 50% of the beamtime is given to general users (GU) and 50% of the available beamtime (CU time) is assigned to COMPRES. All proposals are first submitted through the general proposal system at NSLS to compete for GU time. CU time may be assigned to proposals without a sufficiently high rating to obtain GU time but with significant importance in Geosciences, to increase the number of days for a successful GU proposal, or for use by beamline staff. Appendix II below provides an overview of beamline usage statistics.

A persistent problem in the last few years has been wiggler maintenance issues. However, wiggler performance has considerably improved in July, 2014, and we have lost only minimal days due to wiggler problems before NSLS closure.

Beamline Development

We have significantly improved the absolute energy calibration method (Hong, Chen and Duffy, RSI 2012), e.g. a windows-based software has been developed by X. Hong and used at several beamlines, e.g. X17B3, X17C, X17B2 side station. A motorized translation stage has been made employed for fast energy calibration and monitoring at X17B3 station.

We have also improved the Princeton-manufactured short cell for dedicated high-resolution XRD and PDF measurements.

-- Improvements on the KB mirror system for hard X-ray beam focusing. With the help from the X-ray Optics Group of APS, we have removed worn/scratched/worsened Pt coating layer, and recoated the two KB mirrors before the operation of 2014-I cycle. Much better reflection performance has been achieved by using the recoated mirrors.

VI) The high-pressure DAC program at NSLS-II

The National Synchrotron Light Source (NSLS) at Brookhaven National Laboratory ceased operation on September 30, 2014 after 32 years of distinguished operations. NSLS has been home to the successful high-pressure DAC and LVP facilities for over 20 years. The diamond anvil cell program (X17-DAC) has been one of the most productive programs at NSLS in the past decade.

The NSLS is succeeded by the new medium energy (3 GeV) National Light Source II, which will provide world-leading intensity and brightness, and will produce x-rays more than 10,000 times brighter than the original NSLS. As NSLS before, NSLS II will provide light from infrared to hard X-rays for the use scientific experiments. The commissioning of the first set of 6 project beamlines has started and early science experiments are expected for the second quarter of 2015.

As described in detail in last year's annual report and funding request, the separate operations X17-MAP and X17-DAC, have merged into one operation covering the NSLS-II high pressure program and the APS BM-6 large volume press operation. The leadership team is now formed by Weidner, Ehm and Vaughn. In spring 2014 the Photon Sciences Directorate approved a partner user proposal submitted by the Mineral Physics Institute at Stony Brook University and COMPRES. This constitutes the first step to establish a flourishing Earth Science centric high pressure program at NSLS-II.

VII) Planned Activities

Normal Operations have been completed as of September 30, 2014

The X17-DAC program at NSLS successfully operated through the final cycle at NSLS, closing one week before the final shutdown of the NSLS facility on September 30, 2014, due to the failure of X17C front shutter. As shown above, the demand for experiments at X17-DAC remained strong until the end. We have maintained full beamline operations (albeit with reduced staff) up to the NSLS shutdown.

Decommissioning period at NSLS

The decommissioning of the X17B3 and X17C experimental endstations and the support laboratories has started. This will be a substantial task due to the legacy of different operators of the beamline and therefore different "ownership" of the equipment. Preceding the final decommissioning process, we have completed a detailed inventory of the equipment at X17B3, X17C and support laboratories during the December 2013-January 2014 maintenance period at NSLS. This is currently guiding us in identifying the condition of the equipment and the potential owner as well as helping us to identify the parts suitable to transfer to the new operation at XPD at NSLS-II.

Considering the current staff level at X17-DAC and the limited technical support, we anticipate that especially the de-assembly part of the decommissioning process will take considerable time. We expect that the decommissioning and de-assembly effort will last at least until the end of December 2014 and therefore will partially overlap with the move of the high-pressure program to NSLS-II.

Move to NSLS-II

The timeline of the move of the high-pressure program at X17B2/B3/C and the requested budget are covered in the annual report of X17B2 by Donald Weidner.

Commissioning at NSLS-II

After requested cable replacement, we will re-assemble and debug all the useful DAC devices moved to XPD-D hutch from current X17B3 and C endstations. The timeline of the high-pressure program at NSLS-II and the requested budget are covered in the annual report of X17B2 by Donald Weidner., We anticipate that especially the de-assembly part of the decommissioning process, NSLS-II requested cable replacing, re-assembly, debugging and commissioning of the high-pressure program at NSLS-II will take considerable time.

Part II: Multi-Anvil Cell program at NSLS, June, 2014 – September, 2014

Overview

Available MAC beamtime.

The 2013-2014 year is the last year of operation for the National Synchrotron Light Source (NSLS). As one could anticipate, there has been more lost days due to ring or wiggler failure as the maintenance has been gradually reduced for the facility. Still, we had a robust year of science in the COMPRES program and have been pushing forward with new relationships at other beamlines that should minimize the impact of the dark period and leverage a bright future for multi-anvil high pressure research at national synchrotron facilities.

The 'B' portion of the superconducting wiggler beam (X17) supports three hutches, X17B1, X17B2, and X17B3. The X17B2 houses the multianvil facility and X17B3 houses a portion of the diamond anvil cell program. Together B2 and B3 are in use 2/3 of the time and can be run simultaneously. Thus the multianvil system is available 2/3 of the time that the NSLS is operating.

The B2 hutch has a white beam and a monochromatic beam that is generated by a single bounce monochromator. Thus it is possible to operate two high pressure stations on the floor, each receiving beam. The shielding of the mono station has been completed, so that these two stations can now operate simultaneously. We have successfully tested the T-cup and the DT-cup in the side station and all are functioning properly. The T-cup is a 6-8 styled module with 10mm second stage anvils. We have achieved 29GPa pressure in this system with 2 mm truncations in the past. The DT-cup is a modified T-cup with continuous deformation capabilities. These two guideblocks are compressed by a V-8 Paris-Edinburgh 500 ton press frame. The DT-cup has two additional 50 ton jacks to drive the differential rams. Administrative procedures, such as Safety Approval Forms, have been developed and approved by the NSLS. This system is now accepting experiments.

While outside use of the DT cup has not been great, it has served us as a test-bed for the differential-Kawai type of high-pressure deformation equipment. The Kawai system has always outperformed the DIA style system in achieving high pressure. The addition of a differential ram system in the DIA has met resounding success over the last decade providing a machine that can apply a differential stress on a sample at high pressure and temperature. The DT system reconfigures this into a Kawai style apparatus. Our goal is to achieve much higher pressure for differential stress measurements. Indeed, the Kawai geometry has achieved a megabar in the Japanese laboratories and can set the goals of the DT system. At the end of this year, we received the DT25 system that was being built by Rockland Research. While not yet commissioned, this system will be used in the 1000 ton press at the NSLS II as the next step in pushing deformation pressure higher.

Scientific Highlights

Studies by the Yale program at NSLS during 2012-2014 (Karato)

We use RDA (rotational Drickamer apparatus) combined with the synchrotron x-ray facility at X17B2 at NSLS to study the plastic flow behavior of materials under high-pressure and temperature conditions. We have conducted quantitative deformation experiments on two important minerals in Earth's transition zone (410 to 660 km depth). The flow laws (stress-strain rate relationship) of these minerals were investigated using the *in-situ* X-ray diffraction and x-ray radiography. These studies have provided constraints on the resistance of these minerals for plastic flow under a broad range of conditions.

In addition, we have pushed the pressure limit of quantitative studies on plastic flow in order to understand the plastic properties of minerals in the lower mantle (660-2890 km). This is the largest portion of the rocky part of this planet. By analyzing the diffracted x-ray from various portions of the sample, we realized that a substantial pressure gradient is present in the sample assembly of RDA. Consequently, we reduced the sample size to conduct deformation experiments at pressures of ~27 GPa and temperature of ~2100 K (both P and T were determined by the equations of state of two materials). Under these conditions, dominant minerals are $(Mg,Fe)SiO_3$ bridgmanite and (Mg,Fe)O. We found that bridgmanite has substantially higher resistance to deformation than (Mg,Fe)O.

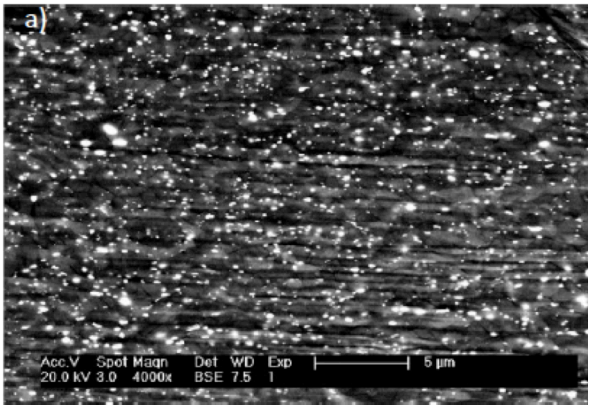

SEM micrograph of a deformed bridgmanite + (Mg,Fe)O aggregate. Dark regions are bridgmanite and light grey regions are (Mg,Fe)O. Bright spots are metallic Fe.

Conditions of deformation are P=27 GPa, T=2130 K, strain-rate ~10^{-5} s^{-1}.

The effect of sintering pressure on anelastictiy of pyrope garnet. (David Dobson, Simon Hunt and Oliver Lord).

Grain-boundary properties affect a diverse range of physical and chemical properties of ceramics, including optical transmission, elastic and viscous properties, partitioning of incompatible elements and electrical conductivity. Despite this, they are a largely neglected aspect of rock- and mineral-physics even though that every rock is a polyscystalline composite (natural ceramic). Here we investigate the effect of sintering pressure on anelasticity of pyrope garnet.

Garnets were synthesized from $Mg_3Al_2Si_3O_{12}$ glass at 1273 K for 24 h at pressures of between 4 and 15 GPa. The mean grain size was ~2 μm for all samples but those recovered from 15 GPa ware white while those recovered from lower pressures were grey-black. Cored

cylinders of pyrope were compressed to 2.5 GPa and subjected to sinusoidally time-varying microstrains in the D-Dial press installed at X17B2 beamline of the NSLS: stress was determined using the length variation of a corundum proxy placed in series with the pyrope sample. The figures below show apparent Young's moduli based on Maxwell viscoelastic fits to the stress-strain data: (A) is for samples annealed at different pressures, all at a driving period of 160s and (B)is for the sample annealed at 4 GPa across a range of driving periods (10-360 s). All samples start off in agreement with the single-crystal average at low temperature and show viscoelastic softening ta the annealing temperature (1273 K) as is common for ceramics. At higher temperatures only the samples sintered at 10 and 15 GPa show significant recovery; the sample sintered 4GPa shows strong dispersion.

The present results show that anelastic behavior is strongly sensitive to sintering pressure, even if the anelasticity measurements are performed under identical conditions. The most likely explanation is that elastically-accommodated grain-boundary sliding is inhibited by strong intergranular bonding at high sintering pressures. This implies that studies which seek to interpret seismic Q values of the lower mantle and inner core (at pressures of 20-360 GPa) on the basis of low-pressure anelasticity measurements are likely to be erroneous.

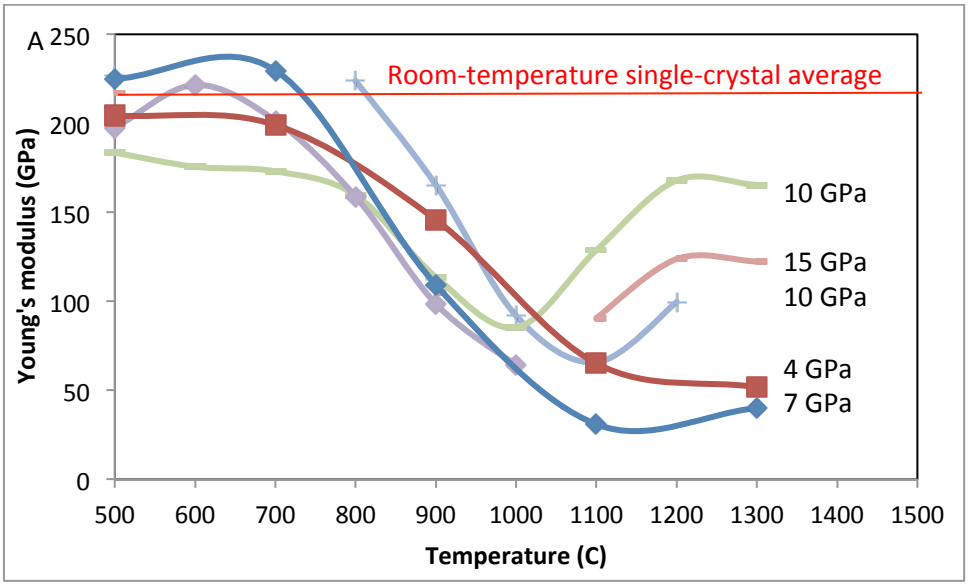

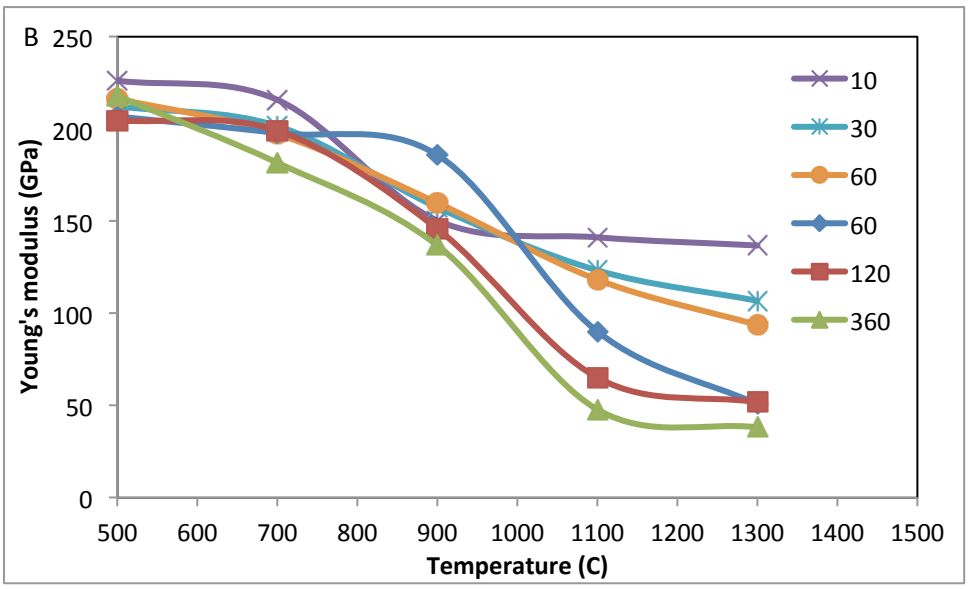

Grain-boundary Plasticity in Olivine (P. Raterron, C. Bollinger*, N. Hilairet, S. Merkel)

The rheology of the Earth upper mantle is controlled by the plasticity of olivine-rich rocks. Olivine single crystal plasticity is understood and quantified to mantle pressures and temperatures (e.g., Bai et al., 1991, JGR, 96, 2441-2463; Raterron et al., 2012, PEPI, 200-201, 105-112). The plasticity of aggregates involves complex mechanisms, and the fundamental question of the amount of strain accommodated at grain boundaries remains unanswered.

Using reported experimental data on San Carlos olivine deformation at mantle conditions - mostly obtained in the D-DIA that equipped the NSLS X17B2 beamline (e.g., Durham et al., 2009, PEPI, 172, 67-73; Bollinger et al., 2014, PEPI, 228, 211-219) - we compared the plasticity of olivine aggregates to that of single crystals and demonstrated that strain at grain boundaries can be orders of magnitude larger than intracrystalline strain. We further showed that the proportion of grain-boundary strain decreases with increasing temperature and stress. Applied along mantle geotherms (Figure), our results shows that grain boundary plasticity is dominant in the shallow mantle. In the deep upper mantle, grain boundary plasticity vanishes and strain is accommodated within the grains.

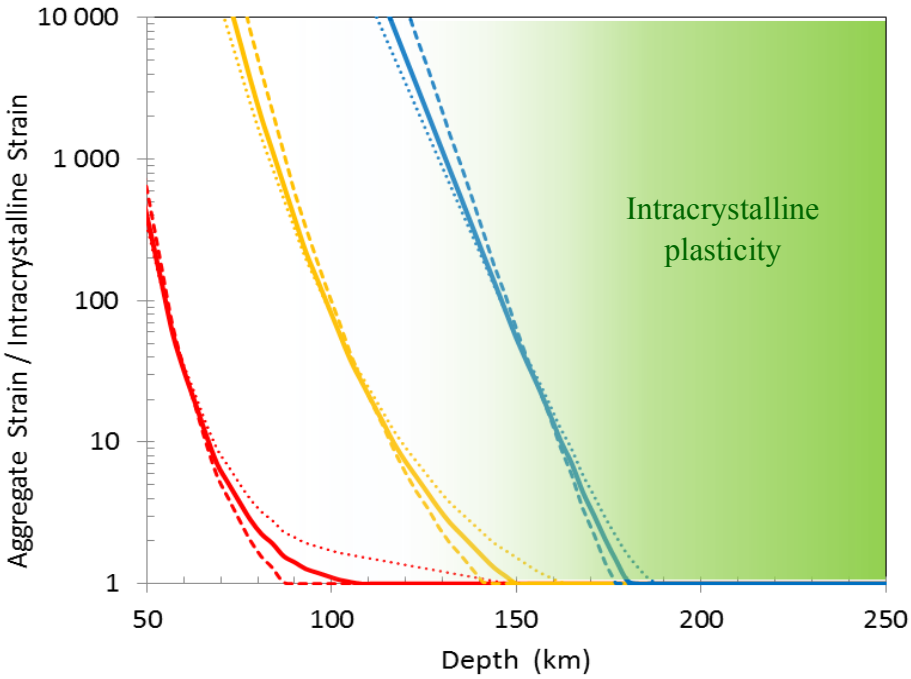

Figure: Aggregate strain / Intracrystalline strain in olivine versus depth, along a 20-Ma (red) and an 80-Ma (yellow) ocean geotherm, and a continental geotherm (blue). The lines correspond to different oxygen fugacities (dotted IW, plain FQM-2, dashed FQM).

Deformation T-Cup: a new controlled strain-rate high-pressure deformation apparatus (Simon Hunt, Richard McCormack, Edward Bailey, Matthew Whittaker, David Dobson, Don Weidner, Li Li; Published as: Hunt et al., 2014, Rev. Sci. Inst., 85, 085103)

The X17B2 side-station beam-line has been host to a new style multi-anvil deformation apparatus, based on the widely used 6-8 split-cylinder geometry. This new apparatus has been used in deformation experiments at pressures in excess of 18 GPa at room temperature and 10 GPa at high temperatures.

In 6-8 (Kawai-type) devices the sample assembly is compressed by eight cubic anvils which in turn are confined by 6 outer wedges. In the new apparatus the two cubes which sit along the split-cylinder axis have been replaced by hexagonal cross section anvils (figure 1). Combining these hexagonal-anvils with secondary differential actuators incorporated into the load frame (figure 2), for the first time, enables the 6-8 multi-anvil apparatus to be used for controlled strain-rate deformation experiments to high strains. Testing of the design, both with and without synchrotron-X-rays, has demonstrated the Deformation T-Cup (DT-Cup) is capable of deforming 1–2 mm long samples to over 55% strain at high temperatures and pressures. To date the apparatus has been calibrated to, and deformed at, 18.8 GPa and deformation experiments performed in conjunction with synchrotron X-rays at confining pressures up to 10 GPa at 800 °C.

Post-commissioning, controlled strain-rate experiments, at pressures up to 10 GPa have been performed investigating the relative strength of the SiO_2 polymorphs. In these experiments, each of the SiO_2 polymorphs was deformed with olivine and the strains measured by X-radiography. The strength of the polymorph can then by normalised to that of olivine. These experiments show that the viscosity of stishovite is greater than that of coesite

which is greater than that of quartz. The strength of the minerals therefore increases with the stabilisation pressure.

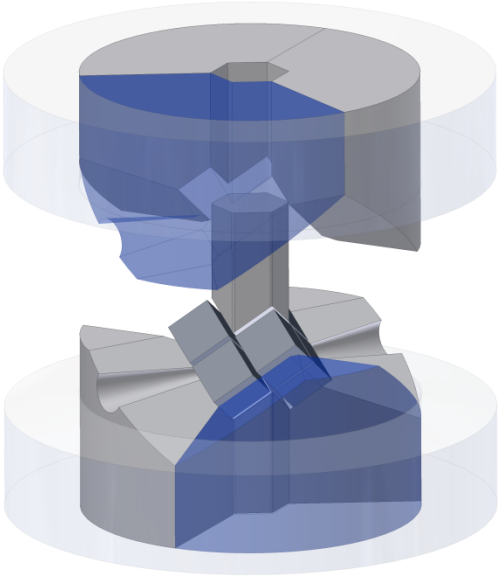

Figure 1: Illustration of the DT-Cup tooling.

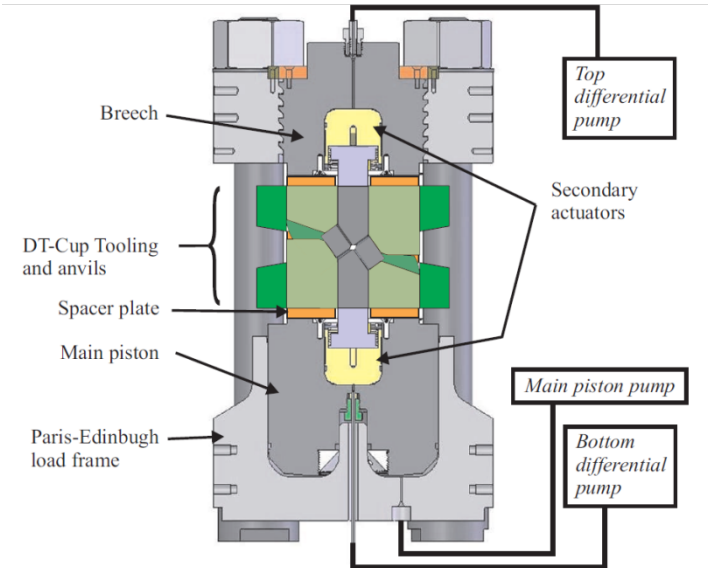

Figure 2: Illustration of Dt-Cup press and tooling.

Experiments: "Compressional anelasticity of HCP metals: a key to the dynamics of Earth's core" (Andrew Walker, University of Leeds)

PASS: 25825

Team: Andrew Walker, Simon Hunt, Ollie Lord, Ed Bailey, Lewis Schardong, Lora Armstrong, Stephen Stackhouse and Matt Whitaker

We undertook two experimental sessions in 2014 with the objective of beginning to constrain the anelasticity of Earth's inner core with a view understanding its microstructure (which would provide information on inner core deformation) and temperature (independently from that available from the melting point iron alloys at extreme pressure). Our proposal included two experimental strands: (a) Measurements of the anelastic response of HPC metal analogues using the D-DIA apparatus installed on the X17B2 beamline. The approach for these experiments follows that described by Li and Weidner (2007; Rev. Sci. Instrum. 78:053902). (b) Direct experiments on HCP iron using the new DTcup installed on the X17B2ss beamline. Although the approach is the same, these experiments would be the first using the new, higher pressure, deformation apparatus.

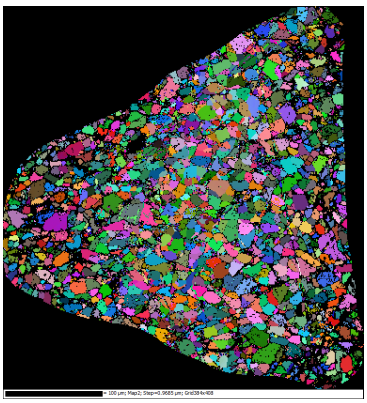

Data from EBSD analysis of recovered Zn sample showing grain orientation (colours relate to Euler angles of crystallographic orientation) and microstructure

The two experimental sessions were marred by machine problems (specifically, problems with the superconducting wiggler's cryogenic system, leading to the loss of around half of the allocated time) but did yield useful insight. Experiments on a zinc analogue show clear evidence for frequency dependent Young's modulus developing at high temperature. Furthermore, the degree of this frequency dependent softening appears to be strongly correlated with the microstructure of the sample, with samples manufactured from packed powder showing less softening than those manufactured from extruded wire. The experiments on HCP iron were less successful. Although we were able to transform iron powder into the high-pressure HCP structure, the DTcup was unable to generate sufficient differential stress to measurably deform the sample at seismic frequencies. Work to understand the cause of this difficulty (which appears to related to an asymmetry in the behavior of the upper and lower differential anvils) is ongoing.

Introducing DIASCoPE: Directly Integrated Acoustic System Combined with Pressure Experiments: System and Design – Matthew L. Whitaker, Kenneth J. Baldwin, William B. Huebsch, Haiyan Chen, Michael T. Vaughan, Donald J. Weidner

Samples and Science – Matthew L. Whitaker, Frederic Bejina, Misha Bystricky, Nicolas Terce

Understanding the properties and behaviors of materials and multi-phase aggregates under conditions of high pressure and temperature is vital to unraveling the mysteries that lie beneath the surface of the planet. Advances in *in situ* experimental techniques using synchrotron radiation at these extreme conditions have helped to provide answers to fundamental questions that were previously unattainable. Synchrotron-based ultrasonic interferometry measurements have proven to be especially important in determining acoustic velocities and thermoelastic properties of materials at high pressures and temperatures. However, due to relatively slow data collection times, it has been difficult to measure the effects of processes as they occur, and instead the measurement is made on the end product of these processes. DIASCoPE is an important step toward addressing this problem.

Over the last three years, we have designed and developed an on-board ultrasonic acoustic velocity measurement system that cuts data collection time down by over an order of magnitude. We can now measure P- and S-wave travel times in samples at extreme conditions in less than one second. Moreover, the system has been fully integrated with the multi-anvil apparatus and the EPICS control system at beamline X17B2 of the National Synchrotron Light Source, allowing for greater ease of control *and* full automation of experimental data collection. The DIASCoPE has completed the testing and commissioning phase, and the first data collected using this powerful new system is presented here.

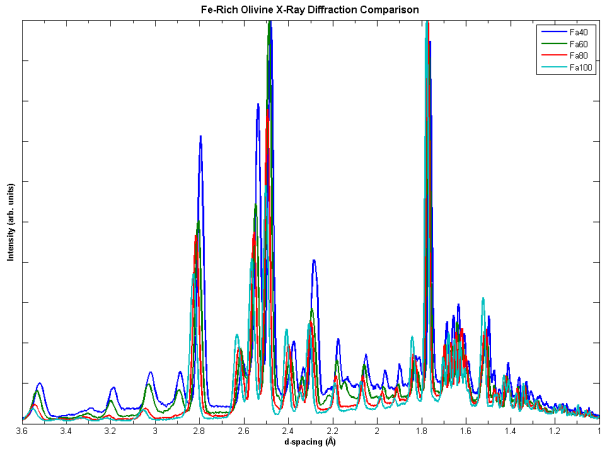

As a collaboration between Stony Brook and Toulouse, we have begun investigating the effects of iron content on the thermoelastic properties and acoustic velocities of iron-rich olivine. While there have been several studies on the Mg-rich side of this solid solution series, there is virtually none on the Fe-rich side, which is something we hope to rectify in this study. Below are three figures showing a very preliminary comparison of the first four samples studied in this investigation: Fa100, Fa80, Fa60, and Fa40. As these figures clearly show, there is a progressive change in d-spacing, P-, and S-wave velocities with Fe content of the olivine.

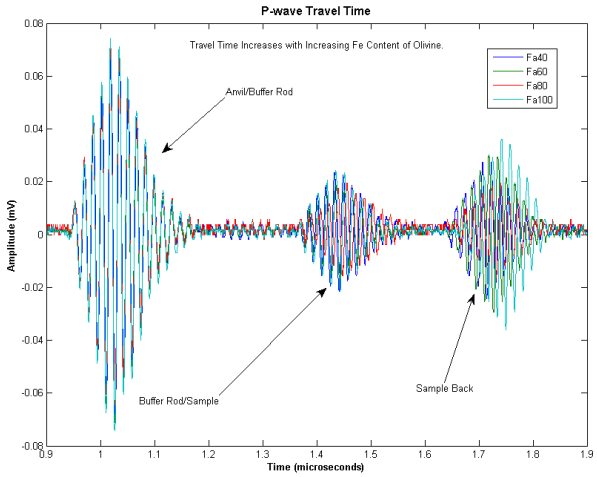

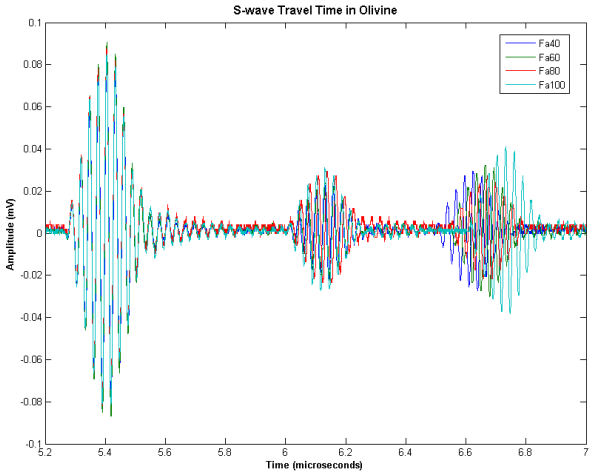

Beamline Support

Personnel		**Funding source**
Matthew Whitaker	beamline scientist	COMPRES
Haiyan Chen	beamline scientist	COMPRES
Michael T. Vaughan	NSLS coordinator	Mineral Physics Institute (Stony Brook U)
Donald J. Weidner	scientist spokesperson	Stony Brook U
Ken Baldwin	software support	Mineral Physics Institute (Stony Brook U)
William Huebsch	part time electronics	COMPRES/Stony Brook

Note: William Huebsch is retired from Stony Brook University and now is employed part-time by the beamline program. Retirement rules limit the salary that we can pay him, yet he works virtually full time.

We have new funding:

- CSEDI Collaborative Research: Grand Challenge for Experimental Study of Plastic Deformation Under Deep Earth Conditions-Weidner, Li, Durham, Wang, Burnley, Karato

We plan to compete for submitting a proposal to the MRI program of NSF for major equipment upgrades for NSLS II.

Beamline Operations – X17MAC

During the final year of operations (10/2013-9/2014), there were:

- 237.5 Operation Days
- 159.25 X17B High Pressure Days (2/3 of 'O' days; X17B2 and X17B3, shared)
- X17B2 Statistics
    - 152.5 days awarded to X17B2 (6.75 days lost to scheduled Wiggler maintenance)
    - 94.5 scheduled operations days usable (58 days lost to Wiggler/ring problems)
    - 10.25 days of unscheduled operations recouped
    - 104.75 days of beamtime actually used in 2013-3, 2014-1, and 2014-2 cycles
- X17B2ss Statistics
    - 142 days awarded to X17B2ss (10.5 fewer days from RDA operations at X17B2)
    - 84 scheduled operations days usable (58 days lost to Wiggler/ring problems)
    - 7.5 days of unscheduled operations recouped
    - 37 days of beamtime actually used in 2013-3, 2014-1, and 2014-2 cycles

Scheduling Breakdown – X17B2

1. (Sep-Dec, 2013) 24 proposals received requesting 101/69 days; 39 days available
   3 granted a total of 9.75 days of General User (Light Source Assigned) time

   11 granted a total of 23.25 days of Contributing User (COMPRES Assigned) time.

   4 days assigned as Beamline Development time; 2 days assigned as Beamline Staff time

2. (Jan-Apr, 2014) 22 proposals received requesting 107/76 days; 38 days available
   4 granted a total of 11 days of General User (Light Source Assigned) time
   12 granted a total of 24.5 days of Contributing User (COMPRES Assigned) time.
   2.5 days assigned as Beamline Development time; 0 days assigned to Beamline Staff
3. (May-Sep, 2014) 20 proposals received requesting 89/63 days; 75.5 days available
   5 granted a total of 21 days of General User (Light Source Assigned) time
   12 granted a total of 45.5 days of Contributing User (COMPRES Assigned) time.
   6 days assigned as Beamline Development time; 2 days assigned as Beamline Staff time

Scheduling Breakdown – X17B2ss

1. (Sep-Dec, 2013) 2 proposals received requesting 12/4 days; 36 days available
   2 granted a total of 10 days of General User (Light Source Assigned) time

   2 granted a total of 2 days of Contributing User (COMPRES Assigned) time.

   24 days assigned as Beamline Development time

2. (Jan-Apr, 2014) 3 proposals received requesting 15/8 days; 35 days available
   2 granted a total of 9 days of General User (Light Source Assigned) time
   2 granted a total of 6 days of Contributing User (COMPRES Assigned) time.
   20 days assigned as Beamline Development time
3. (May-Sep, 2014) 2 proposals received requesting 14/7 days; 71 days available
   1 granted a total of 8 days of General User (Light Source Assigned) time

1 granted a total of 6 days of Contributing User (COMPRES Assigned) time.
57 days assigned as Beamline Development time

For the above scheduling cycles, a total of 74 proposals were submitted to X17MAC. Accounting for repeat submissions, the number of unique proposals received was 47. The NSLS evaluates and rates all proposals, then assigns approximately 25% of the available beamtime. COMPRES then takes these ratings and applies a "COMPRES filter", improving the rating for proposals done by students and on EAR-related projects for assigning the remainder of the time.

<u>One year statistics – X17B2:</u>

Number of beamtime proposals received: **66**

Number of beamtime proposals granted beamtime: **47**

Total number of shifts (days) *requested:* **297/208**

Total number of shifts (days) *granted* **152.5**

Total number of shifts (days) *available* **135**

Subscription rate (= shifts requested / shifts available) **195%/136%**

Number of visits by distinct research groups **53**

Number of unique users **65**

Categorized by affiliation:

University **62** *Private institution* **0**

Gov't Lab/agency **3** *Industry* **0**

Categorized by origin:

USA **49** *Asia* **0**

Canada **0** *Other* **2**

Europe **14**

Total number of person-visits **130 - 40, 45, and 45 for the three cycles**

Number of undergraduate users **1**

Number of graduate student users **25**

Number of visits funded by each funding agency:

NSF **61 (4 half w/ DOE)** *DOE* **37 (4 half w/ NSF)**

DOD **6** *Foreign/Other* **30**

<u>One year statistics – X17B2ss:</u>

Number of beamtime proposals received: **7**

Number of beamtime proposals granted beamtime: **8**

Total number of shifts (days) *requested:* **41/19**

Total number of shifts (days) *granted* **44**

Total number of shifts (days) *available* **142**

Oversubscription rate (= shifts requested / shifts available) **29%/13%**

Number of visits by distinct research groups **8**

Number of unique users **10**

Categorized by affiliation:

University **7** *Private institution* **0**

Gov't Lab/agency **3** *Industry* **0**

Categorized by origin

USA **6** *Asia* **0**

Canada **0** *Other* **0**

Europe **4**

Total number of person-visits **19 - 4, 9, and 6 for the three cycles**

Number of undergraduate users **0**

Number of graduate student users **1**

Number of visits funded by each funding agency

NSF **8**

DOD **3**

DOE **0**

Foreign/Other **8**

For numbers of days requested (e.g. 312/202), the first number is the requested number of days, and the second number is the minimum number of days acceptable for the experiment according to the proposal and beam time request. For granting CU time, we generally used 2 as the minimum, unless fewer were requested. With regard to these data, the relevant unit is one full beam day (not shift). Details of the successful proposals, beamtime allocated, and total usage are provided in an appendix. X17B2 and X17B3 operate in parasitic mode, meaning the beam passes through the upstream station ('B2) and can be used by both stations simultaneously, unless the apparatus in 'B2 blocks it (RDA, for a total of 10 scheduled days in 2013). The side station was underutilized because it was under active development through the 2014-1 cycle, when it became fully operational in all of its intended experimental modes.

Note that we have added a metric, namely whether or not the proposed science was Earth Science related (COMPRES mission). We use this metric as a guide to assignment of COMPRES beamtime rather than who the funding agency happens to be. Thus, for example, we do not give a higher weight to US proposals than we do to international users, nor to NSF support as opposed to DOE support.

Performance Metrics

See appendix V in Excel file: MAC2014Report.xls

Beamline Development

- As described above, the pressure range of the RDA system has been extended into the lower mantle and exploited for new rheology information.
- We have developed an ultrasonic system that is totally integrated into the experimental logic system. That is it interfaces smoothly to the VME crates and can be addressed with the control software. This will enable system controlled data gathering at a preset time (for example during a sinusoidal stress data set). The funding for the equipment ($30,000) is from a non-COMPRES NSF grant to Weidner. Whitaker, Heubsch, and Baldwin successfully set the system up.
- We have modified the imaging algorithm to evaluate strain in the lateral direction when using 4 transparent anvils. For a cylindrically symmetric geometry, this yields volume. Our resolution is a few parts in 10^{-5}.

- We have become extensively involved with the COMPRES Cell Assembly Development Project. Since the closure of the Stony Brook Geosciences Machine Shop, which was our userbase's previous source of cell assemblies, Matt Whitaker has developed an aggressive program in conjunction with Kurt Leinenweber at ASU for developing and manufacturing standardized cell assemblies for our multi-anvil program. Three main standard cell types have been developed and are available for users: 1) DIA for non-deformation Equation of State and synthesis studies; 2) D-DIA for deformation experiments; 3) U-DIA for acoustic studies and large sample synthesis/EoS.

Planned Activities

The MAJOR task in this next year is triggered by the closing of the NSLS on October 1, 2014. We plan to split our current system into two working systems. One will be located at APS on a bending magnet (beamline 6), the other at the NSLS II on the damping wiggler (beamline XPD). The APS bending magnet will provide a similar energy spectrum as X17, but at a lower flux. However, we anticipate access to the majority of the beamtime on that line. The purpose of this is to provide our user base with nearly continuous operations on the 'bread and butter' system. Here we will locate a DDIA with a 250 ton press. At NSLS II, a world premier beamline, but with limited time as it is shared with many other programs, we will place our new D-T25, a Kawai styled differential stress guideblock designed for 25 mm cubes. This is a full scale version of the D-Tcup that we have been gaining experience with. Thus, we will be running our state-of-the-art high pressure system with the state-of-the-art x-ray beam. Thanks to the generosity of Harry Green and Pam Burnley, we will have a second DDIA (built at the same time as the DDIA currently in use) that will allow us to have a backup DDIA at the NSLS II. This will give users the option of using the DT25 or the DDIA.

All of the major equipment items are on hand and we can separate the various parts of our current operation. The APS system will be a white beam system, the same that we now use on X17. The NSLS II system will be monochromatic with very high flux and very high resolution (world class in both of these metrics at very high energy).

Our plan involves staging the APS system at Stony Brook . This is to allow a quick installation in Chicago. This process is underway now. We anticipate that installation will be completed by January, 2014. Once APS is up and running, we will focus our development attention on the NSLS II, where we anticipate that we will have nearly a year with little x-ray beam and more normal operations beginning October, 2015, when we will have 20% of the beamtime.

Part III: Future Operation and Development

With the closing of the NSLS, there is a considerable reduction of the beamtime available to high pressure studies. For every minute of ring operation of the NSLS, X17 provided the capacity for three minutes of high pressure beamtime, distributed between multi-anvil DDIA, DTcup, and diamond anvil pressure cells. We have built the framework for the future of this program with the following goals: 1) maintain a workhorse MAC program with sufficient beamtime to support the user program that has risen up around X17, 2) establish a presence at the NSLS II for both MAC and DAC, pursuing the new capabilities of the newest synchrotron in the DOE program, providing beamtime for new styles of experiment as well as the traditional array, and 3) create a new high pressure beamline with 100% dedicated beamtime. We now have in place agreements with the APS and the NSLS II that guarantee beamtime and experimental space for pursuing the first two of these goals, and have an accepted beamline proposal for building a dedicated high pressure beamline (but this is currently not funded).

NSLS-II & APS high pressure programs

At APS we will operate a DDIA on beamline BM6B. This is a bending magnet with about 20% of the flux of X17, but with a very similar spectrum. This will use our white beam conical slit system and provide full use of the DDIA as it has been used at the NSLS. Thus, all of the experiments that have been done with the DDIA system will be available at the APS. We will receive 38% dedicated time and the highest ranked general user proposals that can add an additional 36%. The remainder of the time will be for the types of programs supported by X17B1 in the past. We believe that we will satisfy the COMPRES MAC user community that has been using X17. It will be a couple of years before we can assess whether we have a greater or a lesser user pressure than we have. That is also true for the other program. We may find that we actually have nearly 100% access, or we may feel pressure from the BM6A program.

At the NSLS II we will receive control of 20% of the beamtime plus high scoring general user proposals. This will be shared between MAC and DAC and will be in the D hutch of beamline XPD, a damping wiggler beam. This beamline will have comparable flux to an APS undulator, but less brightness. It will operate in a monochromatic mode.

The MAC program will operate with a DT25 tooling and a DDIA. The new DT25 is a Kawai style multianvil with differential rams replacing the top and bottom anvils. This style has worked well in our DDIA and we anticipate that we can gain the pressure capabilities that a Kawai system can deliver, which is about 3 times that of a DIA. Our DT10 was the first system of this geometry. But it is designed to operate with 200 ton load. The new system should operate to 1000 ton load. While we have the system in hand, it has not been commissioned at this point. Thus, this first year, with little or no beam, we will commission the press and guideblock,

designing anvils, cell assemblies, assembly protocol, and testing the hydraulic systems. A DDIA will be available and interchangeable with the DT25 for experiments needing the beam of the NSLS II and the pressure system of the DDIA.

The DAC system will be the first DAC system on the NSLS II floor and will provide guidance and support facilities for expansion of the DAC to the wide array of beamlines at the NSLS II. We target the DAC setup to include laser heating with diffraction, as well as high energy diffraction, total scattering, and imaging of samples.

For both MAC and DAC experiments we vision time resolved studies that involve time dependent pressure, temperature, and stress fields. Diaphragm DAC's will be used to enable fast pressure variations and high speed detectors for recording the changes in the sample.

NSLS-II & APS high pressure timeline

The first milestones for the move of the NSLS high pressure program to the beamline BM-6 at the APS and to XPD-D at NSLS-II have been reached. Both operations have an approved Partner User Agreement (NSLS-II) and Management Plan (APS) in place, providing the framework for continuity of the program over the next years.

Moving Activities and Roadmap

NSLS-II

Date	**Milestones**
September 2014	End of operation of NSLS
	X17B2 and X17B3 ended operation on August 30.
	X17C operated until the September 23.
September 2014-December 2014	
September 2014	Decommissioning efforts started in September
	X17B2 has made significant progress in the decommissioning. Equipment essential for the APS operation has been moved SBU and is undergoing integration testing.
	X17B3/C decommissioning is progressing

	October 2014	Storage space at NSLS-II for the HP operation has been identified and is currently being prepared to receive X17 equipment.
	November 2014	Start of the move of equipment from NSLS to NSLS-II
	December 2014	Completion of the decommissioning and moving efforts at NSLS. Access to NSLS experimental floor might be restricted afterwards
January-June 2015		
	January-February 2015	Installation of the large volume press and diamond anvil cell base in hutch-D at XPD
	March-April 2015	Cabling of the instrumentation, reconnecting the controls system and testing of the controls.
		Commissioning of motors and drivers without beam
		Establishing and populating a high pressure support laboratory at NSLS-II.
	May 2014	Safety and Readiness Review
	June 2015	Ready to accept beam in hutch D
June-August 2015		Commissioning

APS

Date	**Milestones**
November, 2014	Stage the entire experimental system at Stony Brook, establish safety targets.
December, 2014	Move system to APS
February, 2014	Complete setup and alignment

Technical Upgrades at XPD-D

In the request period only moderate upgrades are planned to the instrumentation. This is not driven by need, but by the restricted budget situation.

MAC

We plan an upgrade of the control system of the large volume press instrumentation to comply with the NSLS-II control standards. This will allow us to integrate the large volume press program tightly into the NSLS-II controls ecosystem. Furthermore, the upgrade would allow us to request support from the photon Science Directorate controls group.

DAC

The diamond anvil cell program is only considering minor upgrades to the instrumentation. We are planning to motorize the sample position of the ruby system and to replace the manual positioning of the DAC sample stack with a motorized version. In order to realize these upgrades, we are currently evaluating the surplus stages and motors from the decommissioning of BNL operated beamlines at NSLS. We might be able to perform these upgrades without any impact on the budget.

Programmatic Developments

MAC

We will develop the DT25 capabilities as discussed above based on the development at X17B2 of the DT10.

DAC

High Energy focusing optics: Over the period of the past two years, we conducted a number of experiments at X17B3 evaluating a X-ray focusing scheme based on multi-stripe grated multilayer mirrors in KB geometry. Our progress has been reported in the past two annual reports and we have made significant progress increasing photon flux on the sample and reducing the focal spot size. The encouraging results have started an informal R&D collaboration between the diamond anvil cell program, the XPD team and the optics group at NSLS-II. We are planning to use the growth chamber for multi-layer optic at Brookhaven to initially grow two striped multilayers, optimized for focusing at 30 and 60 keV. The new multilayer mirrors should be available for testing with the anticipated start of commissioning in June 2015.

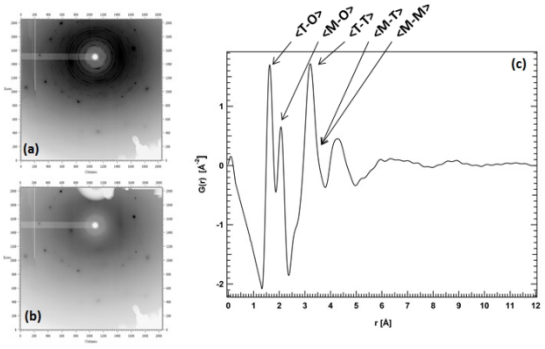

Figure 1 Preliminary diffraction data of Ocean Island Basalt at 14 GPa and about 2400 K. (a) Sample prior to heating showing that the sample is partially crystalline. (b) Fully molten sample at 14 GPa and about 2400 K, remaining powder peaks are from NaCL used as the thermal insulator and pressure medium. (c) PDF derived from the total scattering data in (b), preliminary assignment of the correlations is shown above the maxima in the *G(r)*.

X-ray total scattering: The energy-range provided by XPD (30-70 keV) is ideal to continue and expand our development of X-ray total scattering at high pressure and temperature. The recent publications from X17B3 are demonstrating our leadership in X-ray total scattering at high pressure and the growing user base for this technique. We intend to increase our efforts to couple laser heating with X-ray total scattering in order to perform experiments relevant to melts in the Earth interior. Preliminary experiments on a melt with ocean island basalt composition at 14 GPa and about 2400 K is shown in Figure **1**. The experiments have been conducted at Petra-III in Germany. The flux of the beamline P02.2 at 60 keV is comparable to the expected flux at XPD. We were able to collect data with exposure times of less than 60 s that are suitable for pair distribution analysis. Based on the projected beam characteristic of XPD, we expect that we will be able to perform rapid data collection on molten samples and derive not only structural but density information of the material at high pressure and temperature.

Dynamic compression in MAC and DAC

Static and shock compression represent two extreme cases of pressure generation. While static compression allows access to the isothermal states, shock compression allows access to the thermodynamic states on the principle Hugoniot. However, there is a vast region in the p-V-T-t space that remains inaccessible with either of the two techniques. Bridging this gap has a high potential to reach states and forms of materials that are far from the thermodynamic equilibrium, and potentially have novel and desirable properties.

Besides other groups at synchrotron radiation sources, we have started to develop dynamic compression techniques for the Large Volume Press and the Diamond Anvil Cell. In contrast to shock compression, which allows compression/strain rates in the TPa/s to PPa/s region, we are able to access compression rates of a few MPa/s to 100 GPa/s. While the pilot studies in the LVP led to first transformative scientific results, the dynamic compression in the DAC at NSLS is severely limited due to the comparatively low flux. We will continue the development at XPD at NSLS-II, which will provide a dramatically increased flux for such experiments. This development will help us to overcome the scientific challenges related to understanding of decompression melting, rims of impact craters and the influence of seismic waves on phase equilibrium.

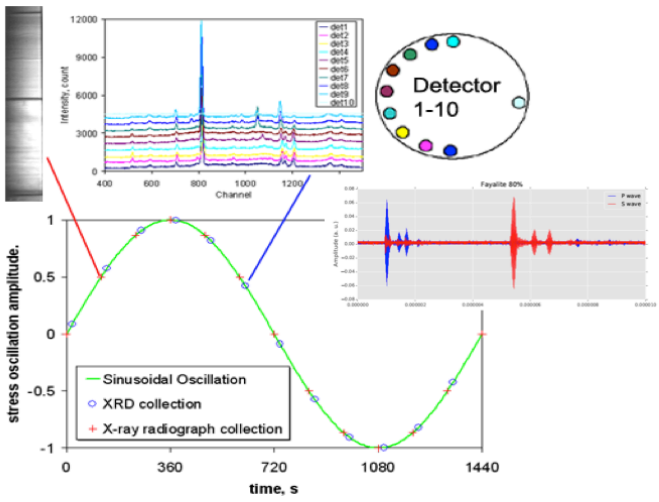

Figure. An example of the type of data now accessible as stress varies sinusoidally with time. The diffraction data can be used to define stress and lattice preferred orientation, the image data can define total strain on the sample and on a stress proxy, ultrasonic data can define the elastic moduli of the sample.

NSLS II in the Context of other US Light Sources

The landscape of storage ring based light sources in the USA is currently going through a dramatic change. The National Synchrotron Light Source (NSLS) ended its operation, NSLS-II just started the commissioning of the first suite of 6 project beamlines and the Advanced Photon Source (APS) and the Advanced Light Source (ALS) are in the planning stages for an upgrade to a diffraction limited sources.

Although the Basic Energy Sciences Advisory Committee (BESAC) of the Department of Energy (DOE) didn't identify the APS or the ALS upgrades as top priorities in their July 2013 report, the planning and the R&D efforts for both upgrades are well advanced [1,2]. The schedule for the APS upgrade proposes a start date of 2018 for the complete decommissioning and new installation of the complete APS storage ring components. The APS leadership developed a very aggressive timetable with a completion of the construction part of the upgrade within one year after the start, followed by a commissioning period of currently undefined length. It is widely perceived that this will probably create a three year cessation of the experimental program at the APS.

The planning for the upgrade of the ALS to ALS-II is at a similar stage of completion. The discussed timelines are not as concrete as the APS timetable yet, but similar dates and durations are discussed. The relatively moderate cost of both upgrade proposals increases the feasibility for DOE to fund both in the proposed time period. This would have a dramatic effect on the US Mineral Physics Community. The APS upgrade will significantly reduce the access to dedicated high pressure experiments for at least two years. After the end of operation of the NSLS high pressure program at the three experimental endstations at X17, the only remaining experimental capabilities would be ALS 12.2.2 and NSLS-II XPD-D. Independent of a potential simultaneous upgrade of ALS to ALS-II, these two high pressure beamlines will not be able to meet the beamtime needs of the Mineral Physics Community in the US.

A number of groups might decide to compete for beamtime at the premier international synchrotron sources during the two year upgrade period. However, the European Synchrotron Radiation Facility and Spring-8 are on track for upgrades starting in 2019 [3], reducing the availability of beamtime for high pressure experiments on a global scale.

It is our belief that COMPRES needs to begin now to assure a continuity of high pressure synchrotron access to the COMPRES community especially during a possible extended period for the APS. The presence of high pressure on the floor of the NSLS II will bolster this effort and the existence of the plans for 4DE, that have been ratified by the NSLS II administration provide a strong starting point. Now, we need to generate a plan for moving forward.

[1] G. Srajer (Deputy Associate Laboratory Director), presentation at Mineral Physics / COMPRES long term strategic planning meeting, Chicago 2014.
[2] H. Tarawneh, C. Steier, R. Falcone, D. Robin, H. Nishimura, C. Sun, W. Wan. ALS-II, a Potential Soft X-ray, Diffraction Limited Upgrade of the Advanced Light Source. Journal of Physics: Conference Series 493 (2014) 012020.
[3] E.S. Reich. Ultimate upgrade for US synchrotron. Nature 501 (2013) 148-149.

Budget

2014-2015 Budget. This is the current years budget. It can be summarized as follows:

	DAC NSLS (1/3 year)	MAC NSLS (1/3 year)	Chicago (2/3 year)	NSLS II (2/3 year)
Technical officer/DAC BL	$26,880.94			$53,762.00
BL scientist/MAC		$25,992.05	$51,984.00	
BL scientist/MAC		$25,497.00		$50,994.00
Fringe Benefits (.41)	$11,021.19	$21,110.51	$21,313.44	$42,949.96
Equipment*	$0.00	$0.00	$20,000.00	$50,000.00
Travel	$1,000.00	$3,000.00	$5,000.00	$2,000.00
Supplies	6075.2346	15392.8895	27079.36	19190.24
Services	$3,500.00			
Shop support		$13,333.33	$30,000.00	$25,000.00
Moving				$20,000.00
IDC (.26) - not equipment	$12,604.11	$27,124.70	$35,197.97	$55,613.01
Totals	$61,081.47	$131,450.48	$190,574.77	$319,509.21
Grand total				$702,615.94

In addition, the President has indicated that we will have $30,500 for APS equipment (a supplement to COMPRES) and up to $20,000 for moving expenses from NY to Chicago.

Unexpected expenses have arisen from needed repairs to the 10 element detector. Canberra informs us that 3 crystals need to be replaced and a few preamps for a cost of about $23,000. We are currently negotiating this and expect to repair it before moving to APS, but the cost will necessarily come from some other category not yet identified.

The 2015-2016 proposed budget is:

	APS	NSLS II	sum
Technical officer/DAC BL, Hong		$82,746.97	$82,746.97
BL scientist/MAC, Chen	$82,746.97		$82,746.97
BL scientist/MAC, Whitaker		$82,746.97	$82,746.97
Electronics, Huebsch		$25,000.00	$25,000.00
Fringe Benefits (.425)	$35,167.46	$80,959.92	$116,127.39
Equipment	$5,200.00	$58,350.00	$63,550.00
Travel	$13,600.00	$7,200.00	$20,800.00
Supplies	$30,473.00	$31,343.00	$61,816.00
Shop support	$45,440.00	$26,720.00	$72,160.00
IDC (.26) - not equipment	$53,931.13	$87,546.38	$141,477.52
	$266,558.56	$482,613.25	$749,171.81
			$749,171.81
Note: salaries are average salary			

Budget Justification

Personnel

Here, the projected salaries represent the average salary of the three scientists without indication of salary distribution among them. Chen will be the beamline scientist at the APS beamline. She will be full time in Chicago.

Whitaker will be the beamline scientist in charge of the multi-anvil program at the NSLS II. He will also be on call for trips to Chicago as needed for the APS program.

Hong will be the beamline scientist in charge of the DAC program at the NSLS II. The main goal of the NSLS II program for this year will be commissioning and beginning user

operation. Responsibilities will expand to bringing DAC activities to other beamlines as the operations become established at XPD.

W. Huebsch is an invaluable member of the beamline team. His expertise is in electronic control systems. He designs, builds, installs, and maintains these systems. He is retired from Stony Brook University and has a limit on his salary, but he works essentially full time. He saves us an incredible amount of money in that he does many tasks that would be very expensive to outsource. Making cables is just one of these tasks and he saves the program 10's of thousands of dollars. His wisdom and advice is broader than electronics and extremely useful.

Equipment

We propose the following equipment acquisition during the next year:

Item	Count/Justification	Chicago	NSLS II
Control upgrade one station (MAC)	This is to upgrade the electronics for one of the stations to the NSLS II standards to allow support of the PSD control group for the high pressure operation. Individual Parts: Moxa ($1850), Delta-Tau Controller (*axis per unit, 32 axis on station ($11000/unit) 4 units for $44000, Scaler $2500, Power Supplies $5000, cables + connectors, $5000.		58350
IsoMet Diamond saw	for sample analysis	5200	
		5200	58350
			63550

We are requesting funds to upgrade the MAC electronics to be compatible with the NSLS II standards. We also request funds for building the user support area of APS.

Travel

Travel expenses are for the following:

Count/Justification	Chicago	NSLS II
COMPRES Annual Meeting 3 scientist + 3 Pis covering transportation to the meeting $800/person	$1,600.00	$3,200.00

Travel and registration for one conference for each of the three beamline scientist $2000/pp	$2,000.00	$4,000.00
Travel SBU-CHI support staff and beamline scientist 10 trips $1000/trip	$10,000.00	
	$13,600.00	$7,200.00
		$20,800.00

Supplies

The requested supplies include the following:

Item	Count/Justification	Chicago	NSLS II
Cold Light Lamp Source	Replacement for broken lamps of binocular microscope (KL 1600)		$1,077.00
Kim Wipes	36 pk normal and XL	$300.00	$341.00
Tweezers	Set of 10	$35.00	$30.00
Cotton-Tipped Applicators	10 Pk	$150.00	$105.00
Methanol/Ethanol/Acetone/Isopropanol	4L bottles	$300.00	$300.00
Turpenoid	4L bottles		$55.00
Needles+Holders	36 ct	$60.00	$100.00
Mounting epoxy Stycast	Single use portions 60 uses		$648.00
Agate Mortar and Pestle sets	2	$180.00	$180.00
Diamonds (DAC)	6 anvils ($650/anvil)		$3,900.00
Gasket material	Rhenium (50 mmx50mm), Tungsten (100 mmx100 mm)		$1,082.00
Sintered diamond anvils (MAC)	20	$6,750.00	$6,750.00
WC anvils/backing plates	50	$10,000.00	$8,000.00
DIA cells	25 for DIA/50 for DDIA/25 for DT25	$3,500.00	$1,500.00
Type D thermocouple		$1,200.00	$500.00

LSNH cables and connectors	NSLS II safety standards require all new cables that are low-smoke-zero-halogens. This is expensive cabling		$2,000.00
Canberra detector cable and connector	required to due to location of electronics in Chicago	$500.00	
Pressure sensor	2	$1,000.00	$1,000.00
Rack for electronics			$1,000.00
MSC tool set		$2,028.00	
MSC metric tools		$1,711.00	
Stero zoom Microscope		$1,469.00	
Vacuum Oven		$1,290.00	
Prosilica CCD camera	for imaging the sample		$2,775.00
		$30,473.00	$31,343.00
			$61,816.00

Shop Support

Technical support from the DOE facility is requested with the following distribution:

Count/Justification	Chicago	NSLS II
Mechanical ($180/hr) 2hr per week 52 weeks		$18,720.00
Mechanical + electrical ($180/hr) 4 hr per week, 52 weeks	$37,440.00	
Rigging services for moving heavy equipment at hutches	$8,000.00	$8,000.00
	$45,440.00	$26,720.00
		$72,160.00

Technical support will be for several individual jobs required to install and maintain the facilities. They will include the following types of requests:

Create special brackets for mounting

Drill and tap holes for assembly

Build dies for pressing high pressure cells (such as boron-epoxy)
Trouble shoot electronic motor drive issues
Move heavy items around in the hutch (rigging)
Install new equipment
Overhaul hydraulic equipment
Confirm alignment of anvils
Rebuild of the platforms for the K-B-mirror system to reduce vulnerability of the system to vibrations.
Build enclosures for an online ruby system.
Addition of lead-sandwich panels to K-B mirror box to reduce instrument background in diffraction data.

The billing rates include salary, fringe benefits, and overhead at the DOE facility.

Appendicies

Appendix I X17-DAC Publications (January 1, 2013 – October 31, 2014)

(Peer review publications, theses, and technical reports)

2015

Drozd V, Durygin A, Saxena S, Antonov V E and Tkacz M (2015) Properties of Ti_3AlH_6 and Ti_3AlD_6 systems at high pressure studied by synchrotron x-ray diffraction analysis, *Journal of Alloys and Compounds* **619**: 78-81.

2014

Chen H, Burnett J, Zhang F, Zhang J, Paholak H and Sun D (2014) Highly crystallized iron oxide nanoparticles as effective and biodegradable mediators for photothermal cancer therapy, *J. Mater. Chem. B* **2:** 757–65

Chen, S, Yao M, Yuan Y, Ma F, Liu Z, Liu R, Cui W, Yang X, Liu B, Zou B, Cui T and Liu B (2014) Structural transformation of confined iodine in the elliptical channels of $AlPO_4$-11 crystals under high pressure, *Physical Chemistry Chemical Physics* **16 (**18): 8301-8309.

Cong R, Liu X, Cui H, Zhang J, Wang Q, Wu X, Zhu H and Cui Q (2014) Plasma assisted synthesis and high-pressure studies of structural and elastic properties of metal nitrides XN (X=Sc,Y), *CrystEngComm* **16** (19): 3977-3985.

Dong H, Dorfman S M, Wang J, He D and Duffy T S (2014) The strength of ruby from X-ray diffraction under non-hydrostatic compression to 68 GPa, *Phys Chem Minerals* **41** (7): 527-535.

Fan D, Wei S, Ma M, Chen Z, Li B and Xie H (2014) High-pressure elastic behavior of $Ca_4La_6(SiO_4)_6(OH)_2$ a synthetic rare-earth silicate apatite: Apowder X-ray diffraction study up to 9.33 GPa, *Phys Chem Minerals* **41:** 85–90

Hong X, Ehm L and Duffy T S (2014) Polyhedral units and network connectivity in GeO_2 glass at high pressure: An X-ray total scattering investigation, *Applied Physics Letters* **105:** 081904

Hong X, Newville M, Duffy T, Sutton S and Rivers M (2014) X-Ray absorption spectroscopy of GeO_2 glass to 64 GPa, *Journal of Physics: Condensed Matter* **26** (3): 035104.

Huang F, Zhou Q, Li L, Huang X, Xu D, Li F and Cui T (2014) Structural transition of $MnNb_2O_6$ under quasi-hydrostatic pressure, *J. Phys. Chem. C* **118** (33): 19280-19286.

Huang S and Chen J (2014) Equation of state of pyrope-almandine solid solution measured using a diamond anvil cell and in situ synchrotron X-ray diffraction, *Physics of the Earth and Planetary Interiors*, **228**: 88-91.

Huang Y, Huang X, Zhao Z, Li W, Jiang S, Duan D, Bao K, Zhou Q, Liu B and Cui T (2014) Experimental verification of the high pressure crystal structures in NH_3BH_3, *The Journal of Chemical Physics* **140:** 244507

Huang X, Duan D, Li F, Huang Y, Wang L, Liu Y, Bao K, Zhou Q, Liu B and Cui T (2014) Structural stability and compressive behavior of ZrH_2 under hydrostatic pressure and nonhydrostatic pressure, *RSC Advances* **DOI:** 10.1039/C4RA06713D

Lang M, Zhang F, Zhang J, Tracy C L, Cusick A B, von Ehr J, Chen Z, Trautmann C and Ewing R C (2014) Swift heavy ion-induced phase transformation in Gd_2O_3, *Nuclear Instruments and Methods B* **326:**121–5

Li D, Wu X, Jiang J, Wang X, Zhang J, Cui Q and Zhu H (2014) Pressure-induced phase transitions in rubidium azide studied by in-situ x-ray diffraction *Applied Physics Letters* **105:** 071903

Li G, Li Y, Zhang M, Ma Y, Ma Y, Han Y and Gao C (2014) Pressure-induced isostructural phase transition in CaB_4, *RSC Adv.,* **4:** 42523-42529

Li Q, Cheng B, Tian B, Liu R, Liu B, Wang F, Chen Z, Zou B, Cui T and Liu B (2014) Pressure-induced phase transitions of TiO_2 nanosheets with high reactive {001} facets, *RSC Adv.* **4:**12873–7

Li Q, Zhang H, Cheng B, Liu R, Liu B, Liu J, Chen Z, Zou B, Cui T and Liu B (2014) Pressure-induced amorphization in orthorhombic Ta_2O_5: An intrinsic character of crystal, *Journal of Applied Physics* **115**:193512

Machon D, McMillan P F, San-Miguel A, Barnes P and Hutchins P T (2014) Semiconductor clathrates: In situ studies of their high pressure, variable yemperature and synthesis behavior, *The Physics and Chemistry of Inorganic Clathrates* Springer Series in Materials Science ed G S Nolas (Springer Netherlands) pp 91–123

Meng X, Fan J, Bao K, Li F, Huang X, Li Y, Tian F, Duan D, Jin X, Zhu P, He Z, Zhou Q, Gao C, Liu B and Cui T (2014) Structural stability and electrical properties of AlB_2 -type MnB_2 under high pressure, *Chinese Physics B* **23** (1): 016102.

Serra-Crespo P, Dikhtiarenko A, Stavitski E, Juan-Alcañiz J, Kapteijn F, Coudert F-X and Gascon J (2014) Experimental evidence of negative linear compressibility in the MIL-53 metal–organic framework family, *CrystEngComm,*

Sun Y, Chen J, Drozd V, Durigin A, Najiba S and Liu X (2014) Phase boundary of pressure-induced *I4mm* to *Cmc2₁* transition in ammonia borane at elevated temperature determined using Raman spectroscopy, *International Journal of Hydrogen Energy* **39:** 8293–302

Tang R, Li Y, Li N, Han D, Li H, Zhao Y, Gao C, Zhu P and Wang X (2014) Reversible structural phase transition in ZnV_2O_6 at high pressures, *J. Phys. Chem. C* **118**:10560–6

Unterborn, C, J. Kabbes, J Pigott, D Reaman and W Panero (2014) The Role of carbon in extrasolar planetary geodynamics and habitability, *The Astrophysical Journal* **793**(2): 124.

Wu T, Tyson T A, Chen H, Gao P, Yu T, Chen Z, Liu Z, Ahn K H, Wang X and Cheong S-W (2014) Pressure dependent structural changes and predicted electrical polarization in perovskite $RMnO_3$, *arXiv:1403.7998 [cond-mat]*

Xi X, He X-G, Guan F, Liu Z, Zhong R D, Schneeloch J A, Liu T S, Gu G D, Xu D, Chen Z, Hong X G, Ku W and Carr G L (2014) Bulk signatures of pressure-induced band inversion and topological phase transitions in $Pb_{1-x}Sn_xSe$, *Phys. Rev. Lett.* **113**:096401

Xiong Z, Liu X, Shieh S R, Wang F, Wu X, Hong X and Shi Y (2014) Equation of state of a synthetic ulvöspinel, $(Fe_{1.94}Ti_{0.03})TiO_4$, at ambient temperature, *Phys Chem Minerals* **41:** 1–7

Xu H, Li C, He D and Jinag Y (2014) Stability and structure changes of Na-titanate nanotubes at high temperature and high pressure, *Powder Diffraction* **29:**147–50

Yang X, Li Q, Liu R, Liu B, Jiang S, Yang K, Liu J, Chen Z, Zou B, Cui T and Liu B (2014) A novel pressure-induced phase transition in $CaZrO_3$, *CrystEngComm* **16:** 4441-4446

Yang X, Li Q, Liu R, Liu B, Zhang H, Jiang S, Liu J, Zou B, Cui T and Liu B (2014) Structural phase transition of $BaZrO_3$ under high pressure, *Journal of Applied Physics* **115** (12): 124907:1-5

Yu T, Tyson T A, Chen H Y, Abeykoon A M M, Chen Y-S and Ahn K H (2014) Nature of structural changes near the magnetic ordering temperature in small-ion rare earth perovskites $RMnO_3$, *arXiv:1403.4807 [cond-mat]*

Yu T, Tyson T A, Gao P, Wu T, Hong X, Ghose S and Chen Y-S (2014) Structural changes related to the magnetic transitions in hexagonal $InMnO_3$, *arXiv:1406.4405 [cond-mat],* Accepted by *PRB* (10/15/2014).

Zhang J, Cui H, Zhu P, Ma C, Wu X, Zhu H, Ma Y and Cui Q (2014) Photoluminescence studies of Y2O3:Eu3+ under high pressure, *Journal of Applied Physics* **115:** 023502

Zhao J and Yang L (2014) Structure evolutions and metallic transitions in In_2Se_3 under high pressure, *J. Phys. Chem. C* **118:** 5445–52

Zheng, W., Z. C. Feng, J.-F. Lee, D.-S. Wuu, and R. S. Zheng (2014), Lattice deformation of wurtzite $Mg_xZn_{1-x}O$ alloys: An extended X-ray absorption fine structure study, *Journal of Alloys and Compounds*, **582**: 157–160,.

Zou Y, Qi X, Wang X, Chen T, Li X, Welch D and Li B (2014) High-pressure behavior and thermoelastic properties of niobium studied by in situ x-ray diffraction, *Journal of Applied Physics* **116:** 013516

2013

Chang, L., Z. Chen, X. Liu, and H. Wang (2013), Expansivity and compressibility of wadeite-type $K_2Si_4O_9$ determined by in situ high T/P experiments, and their implication, *Phys Chem Minerals*, **40**(1): 29–40,.

Cheng, B. et al. (2013), High pressure phase transition of ZnO/SiO_2 core/shell nanospheres, *Journal of Applied Physics*, ***113***(5): 054314.

Chen G, Li Q, Liu R, Hou Y, Wang J, Dong X, Liu B, Yang X, Yao Z, Tan X, Li D, Liu J, Chen Z, Zou B, Cui T and Liu B. (2013) Structural phase transition and photoluminescence properties of YF_3 and YF_3:Eu^{3+} under high pressure, *Physical Chemistry Chemical Physics* **15 (**45): 19925-19931.

Chen Y, Xi X, Yim W-L, Peng F, Wang Y, Wang H, Ma Y, Liu G, Sun C, Ma C, Chen Z and Berger H (2013) High-pressure phase transitions and structures of topological insulator BiTeI, *J. Phys. Chem. C* **117:** 25677–83

Cong, R., H. Zhu, X. Wu, C. Ma, G. Yin, X. Xie, and Q. Cui (2013), Doping effect on high-pressure behaviors of Sc,Y-doped AlN nanoprisms, *J. Phys. Chem. C*, ***117***(8): 4304–4308.

Dan-Dan, H., G. Wei, L. Na-Na, T. Rui-Lian, L. Hui, M. Yan-Mei, C. Qi-Liang, Z. Pin-Wen, and W. Xin (2013), In-situ high-pressure behaviors of double-perovskite Sr_2ZnTeO_6, *Chinese Phys. B*, **22**(5): 059101.

Fan, D., M. Ma, S. Wei, Z. Chen, and H. Xie (2013), High pressure elastic behavior of synthetic $Mg_3Y_2(SiO_4)_3$ garnet up to 9 GPa, *Advances in Materials Science and Engineering*, 502702.

Han, D. D., W. Gao, N. L, R.-L. Tang, L. Li, Y.-M. Ma, Q.-L. Cui, P.-W. Zhu, and X. Wang (2013), In-situ high-pressure behaviors of double-perovskite Sr_2ZnTeO_6, *Chinese Phys. B*, **22**(5): 059101.

He, Q., X. Liu, B. Li, L. Deng, Z. Chen, X. Liu, and H. Wang (2013), Expansivity and compressibility of strontium fluorapatite and barium fluorapatite determined by in situ X-ray diffraction at high-T/P conditions: significance of the M-site cations, *Phys Chem Minerals*, **40**(4): 349–360.

Hong, X., M. Newville, and T. S. Duffy (2013), High-pressure X-ray absorption fine structure in the diamond anvil cell and its applications in geological materials, *J. Phys.: Conf. Ser.*, **430**(1): 012120

Li, C. Y., Z. H. Yu, H. Z. Liu, and T. Q. Lü (2013), High pressure and high temperature in situ X-ray diffraction study on the structural stability of tantalum disilicide, *Solid State Communications*, **157**: 1–5.

Li, C. Y., Z. H. Yu, H. Z. Liu, and T. Q. Lü (2013), High-pressure powder X-ray diffraction study of Cu_5Si and pressure-driven isostructural phase transition, *Philosophical Magazine Letters*, **93**: 85–92,.

Li, C. Y., Z. H. Yu, H. Z. Liu, and T. Q. Lü (2013), The crystallographic stability and anisotropic compressibility of C54-type $TiSi_2$ under high pressure, *Journal of Physics and Chemistry of Solids*, **74**(9): 1291–1294.

Li, Q., B. Cheng, X. Yang, R. Liu, B. Liu, J. Liu, Z. Chen, B. Zou, T. Cui, and B. Liu (2013), Morphology-tuned phase transitions of anatase TiO_2 nanowires under high pressure, *J. Phys. Chem. C*, **117**(16): 8516–8521.

Liu, G., L. Zhu, Y. Ma, C. Lin, J. Liu, and Y. Ma (2013), Stabilization of 9/10-fold structure in bismuth selenide at high pressures, *J. Phys. Chem. C*, **117**(19): 10045–10050.

Liu, L., H. X. Song, H. Y. Geng, Y. Bi, J. Xu, X. Li, Y. Li, and J. Liu (2013), Compressive behaviors of bcc bismuth up to 55 GPa, *Physica Status Solidi (b)*, **250**: 1398–1403.

Ma, C., H. Cui, F. Li, J. Wang, X. Wu, J. Zhang, Q. Zhou, J. Liu, and Q. Cui (2013), The novel phase transition of $NaBi(WO_4)_2$ under high pressure, *Journal of Solid State Chemistry*, **200**: 246–250.

Ma, M., W. Liu, Z. Chen, Z. Liu, and B. Li (2013), Compression and structure of brucite to 31 GPa from synchrotron X-ray diffraction and infrared spectroscopy studies, *American Mineralogist*, **98**(1): 33–40.

Wei, S., M. Ma, D. Fan, J. Yang, W. Zhou, B. Li, Z. Chen, and H. Xie (2013), Compressibility of mimetite and pyromorphite at high pressure, *High Pressure Research*, **33**(1): 27–34.

Xi, X., C. Ma, Z. Liu, Z. Chen, W. Ku, H. Berger, C. Martin, D. B. Tanner, and G. L. Carr (2013), Signatures of a pressure-induced topological quantum phase transition in BiTeI, *Phys. Rev. Lett.*, **111**(15): 155701.

Xu, Y., H. Zhu, C. Ma, P. Zhu, R. Cong, X. Wu, W. Gao, and Q. Cui (2013), Pressure-induced structural phase transition in AlN:Mg and AlN:Co nanowires, *Journal of Solid State Chemistry*, **202**: 33–37.

Yang, X. et al. (2013), Pressure-induced amorphization in Gd_2O_3/Er^{3+} nanorods, *J. Phys. Chem. C*, **117**(16): 8503–8508.

Zhang F X, Xiao H Y, Lang M, Zhang J M, Zhang Y, Weber W J and Ewing R C (2013) Structure and properties of rare earth silicates with the apatite structure at high pressure, *Phys Chem Minerals* **40**: 817–25

Zhao, J., H. Liu, L. Ehm, D. Dong, Z. Chen, and G. Gu (2013), High-pressure phase transitions, amorphization, and crystallization behaviors in Bi_2Se_3, *Journal of Physics: Condensed Matter*, **25**(12).

Zhao, J., H. Liu, L. Ehm, D. Dong, Z. Chen, Q. Liu, W. Hu, N. Wang, and C. Jin (2013), Pressure-induced phase transitions and correlation between structure and superconductivity in iron-based superconductor $Ce(O_{0.84}F_{0.16})FeAs$, *Inorg. Chem.*, **52**: 8067–8073.

Zhu, H., F. Zhang, C. Ji, D. Hou, J. Wu, T. Hannon, and Y. Ma (2013), Pressure-induced series of phase transitions in sodium azide, *Journal of Applied Physics*, **113**(3): 033511.

Appendix II DAC Beamline Statistics

	Jan 2014 - May 2014		June - Sept 2014			
	X17C	X17B3	X17C	X17B3		
Number of beamtime proposals received*	25	11	21	8		
Number of beamtime proposals granted beamtime	29	12	58	18		
Total number of days requested **	131	56	159	69		
Total number of days granted	59	25	105	49		
Total number of days available	57	23	101	36		
Oversubscription rate (= shifts requested / shifts available)	2.30	2.43	1.57	1.92		
Number of visits by distinct research groups	17	8	27	8		
Number of unique users	31	18	45	20		
University	14	5	22	8		
Gov't Lab/agency	3	3	7	2		
Industry	0	0	0	0		
USA	7	7	14	7		
Canada	1	1	1	1		
Europe	0	0	0	0		
Israel	1	0	1	0		
Asia	8	0	11	2		

Total number of person-visits	35	20	53	25
Number of undergraduate users	2	2	2	1
Number of graduate student users	9	6	6	3
Number of visits funded by each funding agency**				
NSF	1	4	6	5
DOD	1		3	1
DOE	3	2	4	1
Foreign/Other	11	1	13	4

	Jan 2013 - May 2013		June - Aug 2013		Sept - Dec2013	
	X17C	X17B3	X17C	X17B3	X17C	X17B3
Number of beamtime proposals received*	17	10	21	12	25	15
Number of beamtime proposals granted beamtime	38	16.5	37	11	29	11
Total number of days requested **	81	46	108	61	117	68
Total number of days granted	70	36	72	36	59	24
Total number of days available	65	25.5	68	31.5	61	25
Oversubscription rate (= shifts requested / shifts available)	1.25	1.8	1.59	1.94	1.92	2.72
Number of visits by distinct research groups	16	7	21	6		
Number of unique users	27	13	37	19		

University	11	6	12	6
Gov't Lab/agency	5	1	5	1
Industry	0	0	0	0
USA	10	6	9	4
Canada			1	
Europe			1	1
Asia	6	1	8	1
Total number of person-visits	28	15	40	21
Number of undergraduate users	0	0	0	0
Number of graduate student users	14	8	16	9
Number of visits funded by each funding agency**				
NSF	2	4	1	2
DOD	0			
DOE	7	3	7	2
Foreign/Other	7	1	12	2

Appendix III Beamtime Schedule and Proposals Received

X17C Schedule

2013-I

PI Name	Proposal	Assigned Time	Coments
Wiggler Warmup		1/16 (0:00)-2/6(12:00)	No Beam
ADXD Setup		2/6(12:00)-2/8(12:00)	
Qiliang Cui	19484	2/8 (12:00)-2/11(12:00)	
Trevor Tyson	21409	2/14 (12:00)-2/18(12:00)	
Matthew Whitaker	22259	2/18 (12:00)-2/20(12:00)	
Jiuhua Chen	19439	2/20 (12:00)-2/25(6:00)	
Liuxiang Yang	23035	2/26 (12:00)-3/1(12:00)	

Michael Kruger	22962	3/1 (12:00)-3/4(6:00)	
Changqing Jin	23004	3/6 (12:00)-3/11(12:00)	
Yanzhang Ma	21248	3/14 (12:00)-3/18(12:00)	
Itzhak Halevy	23145	3/18 (12:00)-3/21(12:00)	
Maining Ma	17820	3/21 (12:00)-3/25(6:00)	
Maik Lang	23211	3/26 (12:00)-3/30(12:00)	
Bingbing Liu	22005	3/30 (12:00)-4/1(12:00)	
Quanjun Li	21238	4/3 (0:00)-4/5(19:00)	
Chunli Ma	21973	4/5 (20:00)-4/8(12:00)	
Chunli Ma	21973	4/11 (12:00)-4/15(6:00)	
Xin Wang	22076	4/16 (12:00)-4/21(12:00)	
EDXD Setup		4/21 (12:00)-4/24(12:00)	
Jinfu Shu	22973	4/24 (12:00)-4/29(12:00)	

2013-II

PI Name	Proposal	Assigned Time	Coments
Jinfu Shu	CU:22973	05/01 (12:00) - 05/0512:00)	
ADXD Setup		06/05 (08:00) - 06/08 (12:00)	
Xuefei Li	CU:23241	06/08 (12:00) - 06/11 (12:00)	
Davide Levy	GU:23968	06/11 (12:00) - 06/14 (12:00)	
Trevor Tyson	GU: 21409	06/14 (12:00) - 06/17 (06:00)	
Trevor Tyson	CU:19644	06/18 (12:00) - 06/21 (12:00)	
Fenxian Huang	CU:24012	06/21 (12:00) - 06/24 (12:00)	
Maining Ma	CU:20005	06/26 (00:00) - 06/27 (12:00)	
Dawei Fan	GU:23528	06/27 (12:00) - 07/01 (06:00)	

Quanjun Li	GU:21238	07/13 (12:00) - 07/18 (12:00)	
Sean Shieh	CU:24130	07/18 (12:00) - 07/22 (06:00)	
Changqing Jin	GU:23004	07/23 (12:00) - 07/26 (12:00)	
Wei Gao	CU:24075	07/26 (12:00) - 07/29 (06:00)	
Chuanli Ma	GU:21973	07/31 (12:00) - 08/05 (12:00)	
Yanzhang Ma	GU:21248	08/08 (12:00) - 08/12 (12:00)	
Yongzhou Sun	GU:20795	08/13 (12:00) - 08/16 (12:00)	
Yongzhou Sun	GU:22487	08/16 (12:00) - 08/19 (06:00)	
Liuxiang Yang	GU:23035	08/19 (12:00) - 08/24 (12:00)	

2013-III

PI Name	Proposal	Assigned Time	Coments
Setup		09/13 (12:00) - 09/14 (12:00)	
Xuefei Li	CU:23241	09/14 (12:00) - 09/18 (12:00)	

Trevor Tyson	GU:21409	09/19 (12:00) - 09/23 (06:00)	
Dawei Fan	CU:23528	09/24 (12:00) - 09/27 (12:00)	
Yan Li	CU:25057	09/27 (12:00) - 09/30 (12:00)	
Meili Wang	CU:25284	10/02 (12:00) - 10/04 (12:00)	
Xin Wang	GU:22076	10/04 (12:00) - 10/07 (12:00)	
Xiaoxiang Xi	GU:25091	10/10 (12:00) - 10/15 (12:00)	
Davide Levy	GU:23968	10/15 (12:00) - 10/18 (12:00)	
Zhongying Mi	CU:25157	10/18 (12:00) - 10/21 (06:00)	
Fei Sun	GU:25079	10/22 (12:00) - 10/25 (12:00)	
Bin Chen	CU:25266	10/25 (12:00) - 10/28 (12:00)	
Lingping Kong	GU:25178	10/30 (12:00) - 11/04 (12:00)	
Gang Liu	GU:25214	11/07 (12:00) - 11/09 (12:00)	

Zhenhai Yu	GU:25182	11/09 (12:00) - 11/11 (12:00)	
Zhiqiang Chen	CU:25246	11/11 (12:00) - 11/14 (12:00)	
Jiuhua Chen	CU:21243	11/14 (12:00) - 11/18 (06:00)	
Jinggeng Zhao	GU:25134	11/19 (12:00) - 11/23 (12:00)	
Maik Lang	GU:23211	11/23 (12:00) - 11/27 (06:00)	

2014-I

PI Name	Proposal	Assigned Time	Coments
Setup		Comissioning days	
Zhiqiang Chen	GU:25246	02/19 (12:00) - 02/24(12:00)	
Yan Li	GU:25057	02/24 (12:00) - 02/27(12:00)	
Xin Wang	CU:22076	2/27 (12:00) - 3/2 (12:00)	
Lei Su	CU:23211	3/2 (12:00) - 3/07 (12:00)	
Liping Huang	GU:26283	03/07 (12:00) - 3/9 (12:00)	

Davide Levy	CU:23968	03/09 (12:00) - 3/14 (12:00)	
Trevor Tyson	CU:21409	3/14 (12:00) - 3/17(12:00)	
Sean Shieh	GU:26314	3/20 (12:00) - 3/25 (12:00)	
Gang Liu	GU:25214	3/25 (12:00) - 3/29 (12:00)	
Zhenhai Yu	GU:25182	3/29 (12:00) - 4/2 (12:00)	
Jinggeng Zhao	GU:25134	4/2 (12:00) - 4/06 (12:00)	
Qiliang Cui	CU:19484	4/6 (12:00) - 4/10 (12:00)	
Quanjun Li	CU:21238	4/10 (12:00) - 4/13 (12:00)	
Xiaoxiang Xi	GU:25091	4/13 (12:00) - 4/19(12:00)	
Yanzhang Ma	CU:26461	4/19 (12:00) - 4/24 (12:00)	
Maining Ma	CU:20005	4/24 (12:00) - 4/27 (12:00)	
Yongzhou Sun	CU:22487	4/27 (12:00) - 4/30 (24:00)	

2014-II

PI Name	Proposal	Assigned Time	Comments
Setup		05/1 (12:00) - 05/4(12:00)	
BL Optimzation/development	CU	05/7 (12:00) - 05/11(12:00)	
Maik Lang/Fuxiang Zhang	CU	05/23 (12:00) - 05/29(12:00)	
Trevor Tyson	CU	05/29 (12:00) - 06/1(12:00)	
Zhao Jinggeng	GU:25134	06/01 (12:00) - 6/5 (12:00)	
Yu Zhenhai	Gu:25182	6/5 (12:00) - 6/8(12:00)	
Li Chunyu	GU:27016	6/8 (12:00) - 6/13 (12:00)	
Xi Xiaoxiang	GU:25091	6/13 (12:00) - 6/16 (12:00)	
Sean Shiem/Liu Xi	GU:27175	6/18 (12:00) - 6/24 (12:00)	
Halevy_Itzhak	GU:27376	6/24 (12:00) - 6/30 (6:00)	
Hong/Duffy	CU	7/1 (12:00) - 7/6 (12:00)	

Sims Melissa/Lars	GU:27306	7/6 (12:00) - 7/12 (12:00)	
Ma Yanzhang	CU	7/12 (12:00) - 7/15 (12:00)	
Liu_Bingbing	GU:2205	7/17 (12:00) - 7/22 (12:00)	
Davide Levy	GU:27057	07/22 (12:00) - 7/25 (12:00)	
Kong Lingping	GU:25178	07/25 (12:00) - 7/30 (12:00)	
Lars Ehm	CU	07/30 (12:00) - 7/31 (18:00)	
Chen Bin	GU:26492	8/1 (18:00) - 8/05 (12:00)	
Ma Yanzhang	GU:26546	8/6 (0:00) - 8/12 (6:00)	
Mi Zhongying	GU:27283	8/14 (12:00) - 8/18 (12:00)	
Maining Ma/Baosheng Li	CU	8/18 (12:00) - 8/21(12:00)	
Wu Qinghua	GU:27113	08/21 (12:00) - 08/26(12:00)	
Xu Zhishuang	GU:26329	8/26 (12:00) - 9/3 (12:00)	

Zhu_hongyang	GU:24066	9/3 (12:00) - 9/6 (12:00)	
Cui Qiliang	CU	9/6 (12:00) - 9/8 (12:00)	
Zhu Pingwen	CU	9/10 (12:00) - 9/14 (0:00)	
Li Yan	CU	9/14 (0:00) - 9/17 (0:00)	
Wang Xin	CU	9/17 (0:00) - 9/19 (12:00)	
Su Lei	CU	9/19 (12:00) - 9/22 (12:00)	

X17C Proposals Received

2013-I

Form #	PI Name	Institution	Title	Funding
17820	Maining Ma	Graduate University of the Chinese Academy of Sciences	Study on Equation of State of Natural Mantel Minerals	Foreign
19484	Qiliang Cui	Jilin University	Pressure-induced phase transition of rare earth doped III-nanonitride Diluted Magnetic Semiconductor(DMS)	foreign
21238	Quanjun Li	Jilin University	Pressure induced metal-insulator transition in VO2 bulks and nanomaterials	foreign
21248	Yanzhang	Texas Technical	The high pressure transformations of azides-	Other

	Ma	University	searching for high energetic materials	(DTRA)
21409	Trevor Tyson	New Jersey Institute of Technology	Exploring Electric Polarization Mechanisms in Multiferroic Oxides: High Pressure Structures	DOE
21973	Chunli Ma	Jilin University	High pressure X-ray diffraction studies of cyclopentane	foreign
22005	Bingbing Liu	Jilin University	High pressure PDF study of polymorphism in TiO2 nanomaterials	Foreign
22076	Xin Wang	State Key Laboratory of Superhard Materials	Crystal structures of doped vanadates R[SUB]1-x[/SUB]A[SUB]x[/SUB]VO[SUB]3[/SUB] at high pressures	Foreign
22258	Matthew Whitaker	SUNY @ Stony Brook	Acoustic Velocities and Thermoelastic Properties of Iron/Light-Element Alloys at High Pressure and Temperature	NSF
22259	Matthew Whitaker	SUNY @ Stony Brook	Acoustic Velocities and Thermoelasticity of Deep Crustal and Mantle Minerals at High Pressure and Temperature	NSF
22487	Yongzhou Sun	Florida International University	Interaction of Lithium amidoborane and nanoconfined hydrogen at high pressureammonia borane with	DOE
22962	Michael Kruger	Materials Science & Condensed Matter Physics	High Pressure XRD Study of Molybdates and Tungstates	
22973	Jinfu Shu	Carnegie Institution of Washington	Single Crystal X-ray Diffraction Study of Minerals from Tibet, China	DOE
23004	Changqing Jin	Chinese Academy of Sciences, Institute of Physics	Pressure tuned structure evolution of novel quantum matters	Foreign
23035	Liuxiang Yang	Carnegie Institution of Washington	Structural and Tc evolution of Cuprate superconductors under pressure	DOE
23145	Itzhak Halevy	Nuclear Research Center Negev, NRCN	The Fe-Cr system, crystallographic and magnetic phase diagram underhigh-Pressure and temperature.	DOE

23211	Maik Lang	University of Michigan	Response of Minerals to Extreme Conditions of Ion Irradiation and High Pressure: A Novel Approach in Geosciences	DOE
19439	Jiuhua Chen	Florida International University	Grain boundary effect on elasticity of mantle minerals through equation of state	NSF

2013-II

Form #	PI Name	Institution	Title	Funding
23968	davide levy	University of Tel Aviv	behaviour of energetic materials at High Pressure: DTiW	Foreign
23528	Dawei Fan	Institute of Geochemistry@CAS	Effect of hydration on the elastic properties of pyrope at high pressures	NSF-China
21409	Trevor Tyson	New Jersey Institute of Technology	Exploring Electric Polarization Mechanisms in Multiferroic Oxides: High Pressure Structures	DOE
19644	Trevor Tyson	New Jersey Institute of Technology	Exploring Electric Polarization Mechanisms in Multiferroic Oxides: High Pressure Structures	DOE
24130	Sean Shieh	Western University	High Pressure and High Temperature Study on Iron and Manganese Spinel	Other (NSERC)
21973	Chunli Ma	Jilin University	High pressure X-ray diffraction studies of cyclopentane	foreign
24012	Fengxian Huang	Jilin University	High-Pressure X-ray Diffraction Studies of MgTa2O6	Foreign
24075	Wei Gao	Jilin University	In situ high pressure XRD studies on lanthanum germanate	Foreign
20795	Yongzhou Sun	Florida International University	In situ IR spectroscopy of ammonia borane confined in MOFs and SBA-15 at high temperature and high pressure	DOE
22487	Yongzhou Sun	Florida International University	Interaction of Lithium amidoborane and nanoconfined hydrogen at high	DOE

			pressureammonia borane with	
21238	Quanjun Li	Jilin University	Pressure induced metal-insulator transition in VO2 bulks and nanomaterials	foreign
23004	Changqing Jin	Chinese Academy of Sciences, Institute of Physics	Pressure tuned structure evolution of novel quantum matters	Foreign
23241	xuefei li	Jilin normal University	Pressure-induced phase transition in ZnO nanostructure and doped ZnO	Foreign
23607	Jafar Al Sharab	Rutgers University	Structural Analysis of Nanostructured Y2O3 and TiO2 materials	Other (University)
23035	Liuxiang Yang	Carnegie Institution of Washington	Structural and Tc evolution of Cuprate superconductors under pressure	DOE
20005	Maining Ma	University of Chinese Academy of Sciences	Study on Equation of State of Natural Garnets	Foreign
21248	Yanzhang Ma	Texas Technical University	The high pressure transformtions of azides-searching for high energetic materials	Other (DTRA)
22973	Jinfu Shu	Carnegie Institution of Washington	Single Crystal X-ray Diffraction Study of Minerals from Tibet, China	DOE

2013-III

Form #	PI Name	Institution	Tittle	Funding
23968	davide levy	University of Tel Aviv	behaviour of energetic materials at High Pressure: DTiW	Foreign
25109	davide levy	University of Tel Aviv	behaviour of two precursors of energetic materials at High Pressure: HBIW and HAIW	Foreign
22076	Xin Wang	State Key Laboratory of Superhard Materials	Crystal structures of doped vanadates R[SUB]1-x[/SUB]A[SUB]x[/SUB]VO[SUB]3[/SUB]	Foreign

			at high pressures	
23528	Dawei Fan	Institute of Geochemistry@CAS	Effect of hydration on the elastic properties of pyrope at high pressures	NSF-China
25157	Zhongying Mi	Western University	Effect of Water on the Texture Development of Serpentine to Mantle Pressures	Other (HPSTAR)
21409	Trevor Tyson	New Jersey Institute of Technology	Exploring Electric Polarization Mechanisms in Multiferroic Oxides: High Pressure Structures	DOE
25229	Gang Liu	HPSTAR	High pressure study on crystal structure of ternary ferroelectric relaxor-PbTiO3 with tetragonal and monoclinc phases	Foreign
25208	Lingping Kong	HPSTAR	High pressure X-ray diffraction study of piezoelectric Pb(Yb1/2,Nb1/2)O3–PbTiO3	Foreign
25214	Gang Liu	HPSTAR	High Pressure XRD and IR Study of Polytypically Disordered Nano-ZnS	Foreign
25182	Zhenhai Yu	HPSTAR	In situ high pressure AD-XRD study of the structural evolution behavior of 3d transition metal pnictides	Foreign
23241	Xuefei li	Jilin normal University	Pressure-induced phase transition in ZnO nanostructure and doped ZnO	Foreign
25091	Xiaoxiang Xi	Brookhaven National Laboratory	Pressure-induced topological phase transitions in PbSe, PbTe, and Sb2Se3 studied by X-ray powder diffraction	DOE
23211	Maik Lang	University of Michigan	Response of Minerals to Extreme Conditions of Ion Irradiation and High Pressure: A Novel Approach in Geosciences	DOE
25006	Xiaozhi Yan	HPSTAR	Shape Evolution of Nuclei in The Course of A First-Order Phase Transition in Nano-Titanium	NSF-China
25246	Zhiqiang Chen	SUNY @ Stony Brook	Static compression of KCl and KBr to 1 Mbar	NSF
25134	Jinggeng	Harbin Institute of	Study of structure evolutions of topological	NSF-China

	Zhao	Technology	insulator under high pressure	
25266	Bin Chen	University of California @ Berkeley	Texturing at Nanoscale	Foreign
25178	Lingping Kong	HPSTAR	The Compressibility, Surface Energy, and Phase Stability of Nano-Titania	Foreign
25079	Fei Sun	Institution of Physics Chinese Academy of Science	The pressure effect on the new diluted ferromagnetic semiconductor (BaxK1-x)(Zn1-yMny)2As2	NSF-China
25057	Yan Li	Jilin University @ State Key Laboratory of Superha	The structural behavior of typical metal borides MBn (M = metal, n = 2, 4, 6,and 12) at high pressures	Foreign
24805	Haining Li	Zhengzhou University of Light Industry	In Situ High Pressure Synchrotron X-Ray Diffraction Study of Ionic Liquid	NSF-China
24802	Xiang zhu	Zhengzhou University of Light Industry	In situ X-ray diffraction Study of Multiple Phase Transitions in Low-Melting Ionic Liquid [BMIM][BF4] under High Pressure up to 30GPa	NSF-China
21243	Jiuhua Chen	Florida International University	Elasticity and plasticity of pyrope-almandine garnet solid solution at high pressures	NSF
25176	Zhishuang Xu	University of Chinese Academy of Sciences	The influence of water on elasticity of pyroxene	Foreign
25284	Meili Wang	Peking University	Stability and equation of state of BaCO3 and SrCO3	Foreign

2014-I

Form #	PI Name	Institution	Tittle	Funding
2000	Maining	University of Chinese Academy of	Study on Equation of State of Natural	Foreign

5	Ma	Sciences	Garnets	
21409	Trevor Tyson	New Jersey Institute of Technology	Exploring Electric Polarization Mechanisms in Multiferroic Oxides: High Pressure Structures	DOE
21973	Chunli Ma	Jilin University	High pressure X-ray diffraction studies of cyclopentane	foreign
22076	Xin Wang	State Key Laboratory of Superhard Materials	Crystal structures of doped vanadates R[SUB]1-x[/SUB]A[SUB]x[/SUB]VO[SUB]3[/SUB] at high pressures	Foreign
22487	Yongzhou Sun	Florida International University	Interaction of Lithium amidoborane and nanoconfined hydrogen at high pressureammonia borane with	DOE
23035	Liuxiang Yang	Carnegie Institution of Washington	Structural and Tc evolution of Cuprate superconductors under pressure	DOE
24066	Hongyang Zhu	Jilin University	High Pressure Synchrotron X-ray diffraction studies on Ammonium Azide	Foreign
24510	Itzhak Halevy	Nuclear Research Center Negev, NRCN	The Fe-Cr-H system, crystallographic and magnetic phase diagram under high-Pressure	DOE
25057	Yan Li	Jilin University @ State Key Laboratory of Superha	The structural behavior of typical metal borides MBn (M = metal, n = 2, 4, 6,and 12) at high pressures	Foreign
25091	Xiaoxiang Xi	Brookhaven National Laboratory	Pressure-induced topological phase transitions in PbSe, PbTe, and Sb2Se3 studied by X-ray powder diffraction	DOE
25109	Davide Levy	University of Tel Aviv	behaviour of two precursors of energetic materials at High Pressure: HBIW and HAIW	Foreign
25134	Jinggeng Zhao	Harbin Institute of Technology	Study of structure evolutions of topological insulator under high pressure	NSF-China
25178	Lingping Kong	HPSTAR	The Compressibility, Surface Energy, and Phase Stability of Nano-Titania	Foreign
2518	Zhenhai	HPSTAR	In situ high pressure AD-XRD study of the structural evolution behavior of 3d	Foreign

2	Yu		transition metal pnictides	
25214	Gang Liu	HPSTAR	High Pressure XRD and IR Study of Polytypically Disordered Nano-ZnS	Foreign
25246	Zhiqiang Chen	SUNY @ Stony Brook	Static compression of KCl and KBr to 1 Mbar	NSF
25266	Bin Chen	University of California @ Berkeley	Texturing at Nanoscale	Foreign
26147	Johanna Nylen	Department of Materials and Environmental Chemistry, Stockholm University	Structure investigation of pressure-amorphized Li2C2 and CaC2	Foreign
26211	Haining Li	Zhengzhou University of Light Industry	In Situ Synchrotron X-Ray Diffraction and Infrared Spectroscopic Study of Ionic Liquid under High Pressure	Foreign
26292	Chunyu Li	Harbin Institute of Technology	AD-XRD investigation on the structural evolution behavior of Bismuth Selenide to Mbar pressures	Foreign
26314	Sean Shieh	Western University	Strength model of Mantle Phases	Other (NSERC)
26329	Zhishuang Xu	Graduate University of the Chinese Academy of Sciences	Study on elasticity of hydrous pyroxene at high pressure and high temperature	Foreign
26357	Bin Chen	HPStar: Center for High Pressure Science and Techn	High Pressure IR and XRD Study of Mix-stacking Nano-ZnS	Foreign
26368	Xiaozhi Yan	HPStar: Center for High Pressure Science and Techn	The Strain Energy in Ho3O2 during Phase Transition	Foreign
26461	Yanzhang Ma	Texas Technical University	High pressure and shear induced phase transition in group III-V nitride	Other US Governmen t (DOD, ARO)

2014-II

Form #	PI Name	Institution	Tittle	Funding
20005	Maining Ma	University of Chinese Academy of Sciences	Study on Equation of State of Natural Garnets	Foreign
21973	Chunli Ma	Jilin University	High pressure X-ray diffraction studies of cyclopentane	foreign
22487	Yongzhou Sun	Florida International University	Interaction of Lithium amidoborane and nanoconfined hydrogen at high pressureammonia borane with	DOE
23528	Dawei Fan	Institute of Geochemistry@CAS	Effect of hydration on the elastic properties of pyrope at high pressures	NSF-China
24066	Hongyang Zhu	Jilin University	High Pressure Synchrotron X-ray diffraction studies on Ammonium Azide	Foreign
25091	Xiaoxiang Xi	Brookhaven National Laboratory	Pressure-induced topological phase transitions in PbSe, PbTe, and Sb2Se3 studied by X-ray powder diffraction	DOE
25109	Davide Levy	University of Tel Aviv	behaviour of two precursors of energetic materials at High Pressure: HBIW and HAIW	Foreign
25134	Jinggeng Zhao	Harbin Institute of Technology	Study of structure evolutions of topological insulator under high pressure	NSF-China
25178	Lingping Kong	HPSTAR	The Compressibility, Surface Energy, and Phase Stability of Nano-Titania	Foreign
25182	Zhenhai Yu	HPSTAR	In situ high pressure AD-XRD study of the structural evolution behavior of 3d transition metal pnictides	Foreign
25218	Gang Liu	HPSTAR	High Pressure XRD and IR Study of	Foreign

			Polytypically Disordered Nano-ZnS	
26329	Zhishuang Xu	Graduate University of the Chinese Academy of Sciences	Study on elasticity of hydrous pyroxene at high pressure and high temperature	Foreign
26492	Bin Chen	HPStar: Center for High Pressure Science and Techn	Copy of High Pressure IR and XRD Study of Mix-stacking Nano-ZnS	Foreign
26546	Yanzhang Ma	Texas Technical University	High pressure and shear induced phase transition in group III nitride	Other US Government (DOD, ARO)
27016	Chunyu Li	HPStar: Center for High Pressure Science and Techn	The structural evolution behavior of Bismuth Selenide under nonhydrostatic conditions up to Mbar pressures	Foreign
27057	Davide Levy	University of Tel Aviv	Energetic materials at High Pressure: 5-aminoterazole and 5-aminoterazolium nitrate	Foreign
27113	Qinghua Wu	SUNY @ Stony Brook	Phase stabilities of pure Ti2C and Ti3C2 compounds under high pressures	National Nuclear Security Administration (NNSA) NSF
27283	Zhongying Mi	HPStar: Center for High Pressure Science and Techn	Water Effect on the Compressibility, Slip and Texture Information of Olivine to Mantle Pressures	Foreign
27306	Melissa Sims	SUNY @ Stony Brook	Detection of Structural Changes in Epidote at High Pressure and Temperature using Powder Diffraction	NSF
27376	Itzhak Halevy	Nuclear Research Center Negev, NRCN	The Fe-Cr-H system, crystallographic and magnetic phase diagram under high-Pressure	DOE
27392	Itzhak Halevy	Nuclear Research Center Negev, NRCN	The Lu2Co17-H and Lu2Ni17-H systems, crystallographic and magnetic phase diagram under high-Pressure	DOE
27397	Trevor	New Jersey Institute	Exploring Electric Polarization Mechanisms in Multiferroic Oxides: High	DOE

	Tyson	of Technology	Pressure Structures	

X17B3 Schedule

2013-I

PI Name	Form	# of Days	Assigned Time
Trevor Tyson	21406	4.5	03/22 (12:00) - 03/27 (0:00)
Lars Ehm	22131	6.5	04/3 (12:00) - 04/9 (12:00)
Bingbing Liu	22005	4.5	03/27 (12:00) - 04/01 (0:00)
Xinguo Hong	22010	3	04/23 (12:00) - 04/27 (12:00)
Anna Plonka	23073	4	04/20 (12:00) - 04/23 (12:00)
Matthew Whitaker	22259	2	04/27 (12:00) - 04/29 (12:00)

Xinguo Hong	20284	5	03/17 (12:00) - 03/22 (12:00)

2013-II

PI Name	Form	# of Days	Assigned Time
Zobel, Mirijam	24084	3	07/15(12:00)-07/18(12:00)
Liu, Bingbing	23073	4.25	07/18(12:00)-07/24(12:00)
Cernova, Natalya	20375	3	07/24(12:00)-07/27(12:00)
Xinguo Hong	24165	6	07/31 (12:00) - 08/8 (12:00)
Trevor Tyson	21406	4.5	08/8(12:00) - 08/12(12:00)
Xinguo Hong	24177	5	08/13(12:00) - 08/18 (12:00)
Lars Ehm	22131	5.75	08/20(12:00) - 08/26(6:00)

2013-III

PI Name	Form	# of	Assigned Time

		Days	
Lars Ehm	25188	6	10/28 (0:00) - 11/5 (0:00)
Xinguo Hong	20284	6	11/07 (12:00) - 11/13 (12:00)
Xinguo Hong	24177	4.5	11/13 (12:00) - 11/18 (0:00)
Beamline Dev.	CU	2	11/19 (12:00) - 11/21 (12:00)
Liping Huang	CU(26283)	2	11/21 (12:00) - 11/23 (12:00)
Jiuhua Chen	CU	2	11/23 (12:00) - 11/25 (12:00)
Wenge Yang	CU	1.5	11/25 (12:00) - 11/27 (12:00)

2014-I

PI Name	Proposal	Assigned Time	Coments
Xinguo Hong	mono/KB system	03/4(12:00) - 03/10(12:00)	
Liping Huang	GU:26283	03/12 (12:00) - 03/15(12:00)	
Hong/Sean Shieh	GU:24165/CU	03/20 (12:00) - 3/26 (12:00)	
Lars Ehm	GU:25188	3/26 (12:00) - 3/29 (12:00)	
Larry Carr	CU:25091	3/29(12:00)-3/31 (6:00)	

Jinlong Zhu	GU:24929	4/1 (12:00) - 4/05 (12:00)	
Chen Jiuhua	CU:21243	4/5 (12:00) - 4/08 (12:00)	
Tom Duffy	GU:24165	04/09 (12:00) - 4/12 (12:00)	
Lars Ehm	GU:25188	4/8 (12:00) - 4/09 (17:00)	
Tom Duffy	CU:22010	04/17 (12:00) - 4/21 (12:00)	

2014-II

PI Name	Proposal	Assigned Time	Coments
80 keV Mono Setup		06/3 (12:00) - 06/8(12:00)	
KB mirror focusing/Beam optimization	CU	06/11 (12:00) - 06/16(12:00)	
Sean Shiem	GU:27338	6/18 (12:00) - 6/24 (12:00)	
Tom Duffy	GU:24165/CU	06/24 (12:00) - 6/29 (12:00)	

Lars Ehm	GU:25188	7/1 (12:00) - 7/7(12:00)	
Trevor Tyson	GU:27397	7/9 (0:00) - 7/15 (6:00)	
Tom Duffy	GU:24165/CU	07/17 (12:00) - 7/27 (12:00)	
Wenge Yang	CU:25261	7/29 (12:00) - 8/1 (12:00)	
Gang Liu	GU:26309	8/1 (12:00) - 8/6 (6:00)	
Tom Duffy	GU:24165/CU	08/6 (12:00) - 8/15 (12:00)	
Yanzhang Ma	26546	08/15(12:00)--09/02 (12:00)	

X17B3 Proposals

2013-I

Form #	PI Name	Institution	Title	Funding
21406	Trevor Tyson	New Jersey Institute of Technology	Exploring Electric Polarization Mechanisms in Multiferroic Oxides: Total Scattering at High Temperature	DOE
22131	Lars Ehm	SUNY @ Stony	Detection and quantification of partial melting in rocks by high pressure and	NSF

		Brook	temperature powder diffraction	
22005	Bingbing Liu	Jilin University	High pressure PDF study of polyamorphism in TiO2 nanomaterials	Foreign
22010	Xinguo Hong	SUNY @ Stony Brook	In-situ laser heating setting up for high-pressure research with diamond anvil cell (DAC) at X17B3 beamline	NSF
22076	Xin Wang	Jilin University	Crystal structures of doped vanadates R1-xAxVO3 at high pressures	Foreign
23073	Anna Plonka	SUNY @ Stony Brook	High pressure doping of tungsten trioxide for photoelectrochemical applications	DOE
22259	Matthew Whitaker	SUNY @ Stony Brook	Acoustic Velocities and Thermoelasticity of Deep Crustal and Mantle Minerals at High Pressure and Temperature	NSF
22962	Michael Kruger	University of Missouri	High Pressure XRD Study of Molybdates and Tungstates	University of Missouri
23109	Dorthe Ravnsbaek	Massachusetts Institute of Technology (MIT)	Electrochemically-Driven Phase Transitions in olivine cathode materials - Materials for lithium-ion batteries	DOE
20284	Xinguo Hong	SUNY @ Stony Brook	Development of laser heating high-pressure pair distribution function (PDF) method with diamond anvil cell (DAC) at X17B3 beamline	NSF

2013-II

Form #	PI Name	Institution	Title	Funding
20375	Natalya Chernova	Binghamton University, SUNY	Pair distribution function analysis of advanced anode materials for Li ion batteries	DOE
21406		New Jersey Institute	Exploring Electric Polarization Mechanisms	DOE

	Trevor Tyson	of Technology	in Multiferroic Oxides: Total Scattering at High Temperature	
22005	Bingbing Liu	Jilin University	High pressure PDF study of polyamorphism in TiO2 nanomaterials	Foreign
22131	Lars Ehm	SUNY @ Stony Brook	Detection and quantification of partial melting in rocks by high pressure and temperature powder diffraction	NSF
22895	Wei Du	SUNY @ Stony Brook	Exsolution of pyrope-grossular garnet	NSF
23968	davide levy	University of Tel Aviv	behaviour of energetic materials at High Pressure: DTiW	Foreign
24084	Mirijam Zobel	University Erlangen	Amorphous-Crystalline Transition of Precursors of ZnO Nanoparticles in Sol-Gel-Processes	Foreign
24130	Sean Shieh	Western University	High Pressure and High Temperature Study on Iron and Manganese Spinel	Foreign
24165	Xinguo Hong	SUNY @ Stony Brook	Structure of disordered materials by X-ray total scattering	NSF
24177	Xinguo Hong	SUNY @ Stony Brook	Equation of states (EOS) of nanomaterials under extreme conditions by X-ray total scattering	NSF
24110	Dorthe Ravnsbaek	Massachusetts Institute of Technology (MIT)	Electrochemically-Driven Phase Transitions in olivine cathode materials - Materials for lithium-ion batteries	DOE
24181	Shanmin Wang	Los Alamos National Laboratory	Structural and magnetic phase transition in MnN under high pressure and temperature	NSF

2013-III

Form #	PI Name	Institution	Title	Funding
20284	Xinguo Hong	SUNY @ Stony Brook	Development of laser heating high-pressure pair distribution function (PDF) method with diamond anvil cell (DAC) at X17B3	NSF

			beamline	
20375	Natalya Chernova	Binghamton University, SUNY	Pair distribution function analysis of advanced anode materials for Li ion batteries	DOE
21406	Trevor Tyson	New Jersey Institute of Technology	Exploring Electric Polarization Mechanisms in Multiferroic Oxides: Total Scattering at High Temperature	DOE
22010	Xinguo Hong	SUNY @ Stony Brook	In-situ laser heating setting up for high-pressure research with diamond anvil cell (DAC) at X17B3 beamline	NSF
23968	davide levy	University of Tel Aviv	behaviour of energetic materials at High Pressure: DTiW	Foreign
24802	xiang zhu	Zhengzhou University of Light Industry	In situ X-ray diffraction Study of Multiple Phase Transitions in Low-Melting Ionic Liquid [BMIM][BF4] under High Pressure up to 30GPa	Foreign
25188	Lars Ehm	SUNY @ Stony Brook	Pressure-induced phase transition mechanisms in relaxor ferroelectrics	NSF
24929	Jinlong Zhu	Los Alamos National Laboratory	Isostructural phase transition driven by cation discontinuous shift of Bi2NiTiO6 compound under high pressure	NSF
25006	Xiaozhi Yan	Sichuan university	Shape Evolution of Nuclei in The Course of A First-Order Phase Transition in Nano-Titanium	Foreign
25107	Sean Shieh	Western University	High Pressure and High Temperature Study on Ca-bearing Silicates	Foreign
25134	Jinggeng Zhao	Harbin Institute of Technology	Study of structure evolutions of topological insulator under high pressure	Foreign
24177	Xinguo Hong	SUNY @ Stony Brook	Equation of states (EOS) of nanomaterials under extreme conditions by X-ray total scattering	NSF
25220	Dorthe Ravnsbaek	Massachusetts Institute of Technology (MIT)	Formation and stability of novel anode materials for high capacity aqueous Na-ion batteries	DOE
25261	Wenge	Carnegie Institution	In-situ high pressure PDF study on core-shell	DOE

	Yang	of Washington	catalysts	
25274	Lin Wang	Carnegie Institution of Washington	Study on the collapsing mechanism of solvated fullerenes using high pressure pair distribution function technique	DOE

2014-I

Form #	PI Name	Institution	Tittle	Funding
24165	Xinguo Hong	SUNY @ Stony Brook	Structure of disordered materials by X-ray total scattering	NSF
24929	Jinlong Zhu	Los Alamos National Laboratory	Isostructural phase transition driven by cation discontinuous shift of Bi2NiTiO6 compound under high pressure	NSF
25134	Jinggeng Zhao	Harbin Institute of Technology	Study of structure evolutions of topological insulator under high pressure	Foreign
25188	Lars Ehm	SUNY @ Stony Brook	Pressure-induced phase transition mechanisms in relaxor ferroelectrics	NSF
25214	Gang Liu	HPSTAR	High Pressure XRD and IR Study of Polytypically Disordered Nano-ZnS	Foreign
26147	Johanna Nylen	Department of Materials and Environmental Chemistry, Stockholm University	Structure investigation of pressure-amorphized Li2C2 and CaC2	Foreign
26249	Xiang Zhu	Zhengzhou University of Light Industry	Structure of Ni-doped ZnO under high pressure	Foreign
26283	Liping Huang	Rensselaer Polytechnic Institute	High energy X-ray diffraction study of pressure-quenched silica glass	NSF
26309	Gang Liu	HPStar: Center for High Pressure	Size effect of interface embrittlement in nano Ni-S system under high pressure	Foreign

		Science and Techn		
26314	Sean Shieh	Western University	Strength model of Mantle Phases	Other (NSERC)
26369	Xinguo Hong	SUNY @ Stony Brook	High pressure PDF measurement for nanomaterials using high energy (80 keV) X-ray microbeam	NSF

2014-II

Form #	PI Name	Institution	Tittle	Funding
22005	Bingbing Liu	Jilin University	High pressure PDF study of polymorphism in TiO2 nanomaterials	Foreign
25188	Lars Ehm	SUNY @ Stony Brook	Pressure-induced phase transition mechanisms in relaxor ferroelectrics	NSF
26309	Gang Liu	HPStar: Center for High Pressure Science and Techn	Size effect of interface embrittlement in nano Ni-S system under high pressure	Foreign
27139	Xiang Zhu	Zhengzhou University of Light Industry	In Situ Synchrotron X-Ray Diffraction and Infrared Spectroscopic Study of Ionic Liquid under High Pressure	Foreign
27175	Sean Shieh	Western University	Deformation and Strength of Zircon at High Pressure and High Temperature	Other (NSERC)
27258	Xinguo Hong	SUNY @ Stony Brook	High resolution radial X-ray diffraction using high-energy X-ray microbeam	NSF
27338	Sean Shieh	Western University	Stability and elasticity of Chromium Spinels	Other (NSERC)
27404	Trevor Tyson	New Jersey Institute of Technology	Ferroelectricity in SrTiO3 nanoparticles: High Resolution X-Ray Diffraction	DOE

Appendix IV MAC publications

Note: This list of publications includes mostly papers that are the direct results of experiments, but some (from Karato group) include publications that use the MAC data for further modeling of the Earth, planets, or materials.

2014

Bollinger, C., Raterron, P., Cordier, P., Merkel, S. (2014), Polycrystalline olivine rheology in dislocation creep: revisiting experimental data to 8.1 GPa, , *Phys. Earth Planet. Int.*, *228, 211-219.*

Chen, J. C., T Yu, S Huang, J Girard, X Liu (2014), Compressibility of Liquid FeS Measured Using X-ray Radiograph Imaging, , *Phys. Earth Planet. Interiors*, *228, 294-299*

Dai, L., Karato, S. (2014), The effect of pressure on hydrogen-assisted electrical conductivity of olivine: implications for the conductivity jump at 410-km, *Phys. Earth Planet. Inter. in press*, *232: 51-56.*

Dai, L., Karato, S. (2014), The effects of Fe and H on the electrical conductivity of olivine, *Phys. Earth Planet. Inter., in press.*

Dai, L., Karato, S. (2014), The effect of oxygen fugacity on hydrogen-assisted electrical conductivity of olivine: implications for the mechanism of conduction, *Phys. Earth Planet. Inter.*, *232: 57-60.*

Dai, L., Karato, S. (2014), High and highly anisotropic electrical conductivity of the asthenosphere caused by hydrogen diffusion in olivine *Earth and Planetary Science Letters, in press.*

Dixon, N. A. (2014), Experimental Constraints on the Rheological Behavior of Olivine at Upper Mantle Conditions, Ph. D. thesis, 125 pp, Massachusetts Institute of Technology.

Du, W., L. Li, and D. J. Weidner (2014), Experimental observation on grain boundaries affected by partial melting and garnet forming phase transition in KLB1 peridotite, *Physics of the Earth and Planetary Interior*(228), 287-293.

Farla, R., Amulele, G., Girard, J., Miyajima, N. and Karato, S., (2014), High pressure and temperature deformation experiments on polycrystalline wadsleyite using the rotational Drickamer apparatus, *submitted to Physics and Chemistry of Minerals*.

Girard, J., G. Amulele, R. Farla, A. Mohiuddin, and S. Karato (2014), In-situ deformation experiments of bridgmanite + (Mg,Fe)O under the lower mantle conditions, *Nature*, *submitted*.

Girard, J. a. K., S. (2014), Evidence and implications of the limited depth range of a metallic-Fe-bearing layer in the lower mantle, *submitted to Nature.*

Hunt, S., A. M. Walker, O. Lord, S. Stackhouse, L. Armstrong, A. Parsons, G. Lloyd and M. Whitaker (2014), Anelasticity of the HCP metal Zinc: a key to understanding the dynamics of Earth's core, abstract DI31A-4252, in *AGU fall meeting*, edited.

Hunt, S. A., A. M. Walker and E. Mariani (2014), Rate of texture development in post-perovskite in *PPV@10 a meeting to celebrate the tenth anniversary of the discovery of post-perovskite.* , edited, Bristol, UK.

Hunt, S. A., Weidner, D. J., McCormack, R. J., Whitaker, M. L., Bailey, E., Li, L., Vaughan, M. T., Dobson, D. P. (2014), Deformation T-Cup: A new multi-anvil apparatus for controlled strain-rate deformation experiments at pressures above 18 GPa. , *Rev. Sci. Instrum.*, *85, 085103*.

Karato, S. (2014), Asymmetric shock heating and the terrestrial magma ocean origin of the Moon, , *Proceedings of the Japan Academy*, *B90: 97-103.*

Karato, S. (2014), Water in the evolution of Earth and other terrestrial planets, Treatise on Geophysics, in *Evolution of the Earth*, edited by e. b. D. J. Stevenson, Elsevier, in press.

Karato, S., Olugboji, T., and Park, J. (2014), Origin of the mid-lithosphere discontinuity, *submitted to Nature Geoscience*.

Karato, S. (2014), Does partial melting explain geophysical anomalies?, *Physics of the Earth and Planetary Interiors*, *228*, 300-306.

Karato, S. (2014), Some remarks on the models of plate tectonics on terrestrial planets: From the view-point of mineral physics, *Tectonophysics*, *631*, 4-13.

Kung, J., B Li. (2014), Lattice Dynamic Behavior of Orthoferrosilite (FeSiO3) toward Phase Transition under Compression, , *J. Phys. Chem. C 118(23),* , 12410-12419

Li, B., R Liebermann (2014), Study of the Earth's Interior Using Measurements of Sound Velocities in Minerals by Ultrasonic Interferometry, *Phys. Earth Planet. Interiors*, *233, 135-153*

Li, L., and D. Weidner (2014), Detection of melting by X-ray imaging at high pressure, *Review of Scientific Instruments*, *doi:10.1063/1.4880730*(85), 4.

Lord, O. T., E. Wan, S. A. Hunt, A. M. Walker, J. Santangeli, M. J. Walter, D. P. Dobson, I. G. Wood, L. Vočadlo, G. Morard and M. Mezouar (2014), The NiSi melting curve to 70 GPa, *Physics of the Earth and Planetary Interiors*, *233, 13-23*.

Miyagi, L., G. Amulele, K. Otsuka, Z. Du, R. Farla, and S. Karato (2014), Plastic anisotropy and slip systems in ringwoodite deformed to high strainin the rotational Drickamer apparatus, *Physics of the Earth and Planetary Interiors*, *228*, 245-253.

Olugboji, T., Park, J., Karato, S., Kawakatsu, H. and Shinohara, M. (2014), The nature of the lithosphere-asthenosphere boundary in the normal oceanic upper mantle *submitted to Geochemistry, Geophysics and Geosystems.*

Otsuka, K., and Karato, S. (2014), The influence of ferric iron and hydrogen on the Fe-Mg inter-diffusion in (Mg,Fe)O ferropericlase in the lower mantle, *Physics and Chemistry of Minerals, in press.*

Raterron, P., Detrez, F.,Castelnau, O., Bollinger C., Merkel, S., Cordier, P. (2014), Multiscale Modeling of Upper Mantle Plasticity: from Single-Crystal Rheology to Multiphase Aggregate Deformation, , *Phys. Earth Planet. Int.*, *228, 232-243.* .

Selway, K. M., Yi, J. and Karato, S. (2014), Water content of the Tanzanian lithosphere: Implications for cratonic growth and stability, *Earth Planet. Sci. Lett.*, *388: 175-186*.

Simon A. Hunt, Donald J. Weidner, Richard J. McCormack, Matthew Whitaker, Edward Bailey, Li Li, Michael T. Vaughan, and D. P. Dobson (2014), Deformation T-Cup: A new apparatus for high temperature controlled strain-rate deformation experiments tested to 18GPa. 2, *Review of Scientific Instruments*, *85*(8), 8.

Wang, S. Y., XH; Zhang, JZ; Zhang, Y; Wang, LP; Leinenweber, K; Xu, HW; Popov, D; Park, C; Yang, WG; He, DW; Zhao, YS (2014), Crystal structures, elastic properties, and hardness of high-pressure synthesized CrB2 and CrB4., *JOURNAL OF SUPERHARD MATERIALS 36, 279-287*

Weidner, D., J., and L. Li (2014), Kinetics of Melting in Peridotite from Volume Strain Measurements, *Physics of the Earth and Planetary Interior*, *submitted*.

Zhang, J., J Han, J Zhu, Z Lin, M Braga, L Daemen, L Wang, Y Zhao (2014), High Pressure-High Temperature Synthesis of Lithium-rich Li3O(Cl, Br) and Li3 − xCax/2OCl Anti-Perovskite Halides *Inorg. Chem. Comm.,*, *48, 140-143*

Zou, Y., X Qi, X Wang, T Chen, X Li, D Welch, B Li (2014), High-pressure Behavior and Thermoelastic Properties of Niobium Studied by in situ X-ray Diffraction, , *J. Appl. Phys.*, *116, 013516*.

2013

Akdogan, E., I Savkliyildiz, H Bicer, W Paxton, F Toksoy, Z Zhong, T Tsakalakos (2013), Anomalous Lattice Expansion in Yttria Stabilized Zirconia Under Simultaneous Applied Electric and Thermal Fields: A Time-Resolved In Situ Energy Dispersive X-ray Diffractometry Study With an Ultrahigh Energy Synchrotron Probe, *J. Appl. Phys.*, *113(23), 233503*

Chen, H., Tian Yu, Peng Gao, Jianming Bai, Jing Tao, Trevor A. Tyson, Liping Wang, and Roger Lalancette (2013), Synthesis and structure of perovskite ScMnO3, *Inorg. Chem.*, *52, 9692-9697*

Deyhim, A., E Every (2013), Development of a Custom High Precision Motion System to Manipulate a 7 Ton Press., *J Phys.: Conf. Ser.*, *425, 132014*

Farla, R., Karato, S., and Cai, Z. (2013), Role of orthopyroxene in rheological weakening of the lithosphere via dynamic recrystallization, *Proc. Nat. Acad. Sci., , 10: 16355-16360*

Girard, J., J Chen, P Raterron, C Holyoke (2013), Hydrolytic weakening of olivine at mantle pressure: Evidence of [100] (010) slip system softening from single-crystal deformation experiments, *Physics of Earth and Planetary Interiors*, *216*, 12-20.

Girard, J., Amulele, G., Mohiuddin, A., Karato, S (2013), Synchrotron deformation experiments of a perovskite + (Mg,Fe)O aggregates under the shallow lower mantle conditions, *EOS, in press*

Grott, M., Baratoux, D., Hauber, E., Sautter, V., Mustard, J., Gasnault, O., Ruff, S., Karato, S., Debaile, V., Knapmeyer, M., Sohl, F., Van Hoolst, T., Breuer, D., Morschhauer, A. and Toplis, M.J. (2013), Long-term evolution of eth Martian crust-mantle system, , *Space Science Review*, *174: 49-111*.

Gwanmesia, G. D., Liping Wang, Adaire Heady, and Robert C. Liebermann (2013), Elasticity and sound velocities of polycrystalline grossular (Ca3Al2Si3O12) at simultaneous high pressures and high temperatures, *Physics of the Earth and Planetary Interiors*, *228, 80-87*

Hunt, S. A., Lindsay-Scott, A., Wood, I. G., Ammann, M. W. and Taniguchi, T (2013), The P-V-T equation of state of CaPtO3 post-perovskite, *Physics and chemistry of minerals*, *40, 73 – 80*.

Hustoft, J., G. Amulele, J. Ando, K. Otsuka, Z. Du, Z. Jing, and S. Karato (2013), Plastic deformation experiments to high strain on mantle transition zone minerals wadsleyite and ringwoodite in the rotational Drickamer apparatus, *Earth and Planetary Science Letters*, *361*, 7-15.

Karato, S., Wang, D. (2013), Electrical conductivity of minerals and rocks in *Physics and Chemistry of the Deep Earth*, edited by S. Karato, pp. 145-182, Wiley-Blackwell.

Karato, S. (2013), Geophysical constraints on the water content in the lunar mantle and its implication for the origin of the Moon, , *Earth Planet Sci. Lett., , 384: 144-153*.

Karato, S. (2013), Theory of isotope diffusion in materials with multiple species and its implications for hydrogen-enhanced electrical conductivity in olivine *Phys. Earth Planet. Inter.*, *219: 49-55.*

Karato, S. (2013), Rheological properties of minerals and rocks, in *Physics and Chemistry of the Deep Earth*, edited by S. Karato, pp. 94-144, Wiley-Blackwell, New York.

Li, L., and D. J. Weidner (2013), Effect of Dynamic Melting on Acoustic Velocities in a Partially Molten Peridotite, *Physics of the Earth and Planetary Interior*, *222*, 1-7.

Miyagi, L., Amulele, G., Otsuka, K., Du, Z. and Karato, S (2013), Large-strain plastic deformation of ringwoodite in the rotational Drickamer apparatus, *Phys. Earth Planet. Inter. in press*.

Olugboji, T. M., Karato, S., and Park, J. (2013), Structures of the oceanic lithosphere-asthenosphere boundary: Mineral physics modeling and seismological signatures, *Geochem., Geophys., Geosyst.*

Otsuka, K., Longo, M., McCammon, C. and Karato, S. (2013), Ferric iron content of ferropericlase as a function of composition, oxygen fugacity, temperature and pressure: Implications for the redox conditions during diamond formation in the lower mantle, *Earth Planet. Sci. Lett.*, *365: 7-16*.

Raterron, P., S Merkel, C Holyoke (2013), Axial temperature gradient and stress measurements in the deformation-DIA cell using alumina pistons, *Review of Scientific Instruments*, *84*(043906).

Savklıyıldız, I., E.K. Akdogan, Z. Zhong, L. Wang, D. Weidner, M. Vaughan, M.C. Croft, and T. Tsakalakos (2013), Phase transformations in hypereutectic MgO-Y2O3 nanocomposites at 5.5GPa, *Journal of Applied Physics*, *113, 203520*

Suer, T.-A. (2013), Olivine viscoelasticity in sinusoidal stress fields at mantle conditions, Stony Brook University.

Wang, D., Karato, S., and Jiang, Z. (2013), An experimental study on the influence of graphite on the electrical conductivity of olivine aggregates, *Geophys. Res. Lett.*

Weidner, D. J., and L. Li (2013), Theory & Practice - Methods for the Study of High P/T Deformation & Rheology, in *Treatise on Geophysics, 2nd Edition*, edited by L. Stixrude and D. P. Geoffrey, Elseviere.

Xu, L., S Mei, NA Dixon, Z Jin, A Suzuki, D.L. Kohlstedt (2013), Effect of water on rheological properties of garnet at high temperatures and pressures, *Earth Planet. Sci. Lett.*, *379, 158-165*

Zhang, J. Z., JL; Velisavljevic, N; Wang, LP; Zhao, YS (2013), Thermal equation of state and thermodynamic Gruneisen parameter of beryllium metal. , *Journal of Applied Physics*, *114, 173509*

Zhu, J., et al (2013), J. Appl. Phys., *J. Appl. Phys.*, *113, 143514*.

2012

Akdogan, E., I Savkhyildiz, B Berke, Z Zhong, L Wang, D Weidner, M Croft, T Tsakalakos (2012), Pressure Effects on Phase Equilibria and Solid Solubility in MgO-Y2O3 Nanocomposites, *J. Appl. Phys.*, *111, 053506* ([98160]).

Bollinger, C., S. Merkel, and P. Raterron (2012), In situ quantitative analysis of stress and texture development in forsterite aggregates deformed at 6 GPa and 1373 K, *Journal of Applied Crystallography*, *45*, 263-271.

Botez, C., R Tackett, J Hermosillo, J Zhang, Y Zhao, L Wang (2012), High Pressure Synchrotron X-ray Diffraction Studies of Superprotonic Transitions in Phosphate Solid Acids *Solid State Ionics*, *213* (58-62).

Dobson, D. P., Richard McCormack, Simon A. Hunt, Michael W. Ammann, Donald Weidner, Li Li, and L. Wang (2012), The relative strength of perovskite and post-perovskite in the system NaCoF3, *Mineralogical Magazine*, *76* 925-932

Girard, J., J. H. Chen, and P. Raterron (2012), Deformation of periclase single crystals at high pressure and temperature: Quantification of the effect of pressure on slip-system activities, *Journal of Applied Physics*, *11, 112607*.

Hunt, S. A., A. M. Walker (2012), Texture development in CaIrO3 post-perovskite., in *European Mineralogical Conference, 1, EMC2012-683.*, edited.

Hunt, S. A., A. M. Walker and D. P. Dobson (2012), Thermal diffusivity of oriented serpentinite at elevated pressures and temperatures by X-radiography, in *EGU General Assembly 2012. Geophysical Research Abstracts, 14, EGU2012-10316.*, edited.

Hunt, S. A., D. R. Davies, A. M. Walker, R. J. McCormack, A. S. Wills, D. P. Dobson, and L. Li (2012), On the increase in thermal diffusivity caused by the perovskite to post-perovskite phase transition and its implications for mantle dynamics, *Earth and Planetary Science Letters*, *319 - 320*, 96-103.

Jing, Z. a. K., S. (2012), Effects of H2O on the density of silicate melts at high pressures: Static experiments and the application of a hard-sphere model of equation of state,, *Geochim. Cosmochim. Acta.*, *85: 357-372*.

Karato, S. (2012), On the origin of the asthenosphere *Earth, Planet. Sci. Lett.*, *321/322: 95-103*.

Li, L., and D. J. Weidner (2012), Anelasticity and Transient Creep in NaMgF3 Perovskite at High Pressure, *Physics of the Earth and Planetary Interior*, *194-195*, 98-106.

McCormack, R. (2012), The Rheological and Transport Properties of Deep Mantle Materials, *Ph.D Thesis. University College London, London*

Otsuka, K. a. K., S. (2012), Deep penetration of molten iron into the mantle caused by the morphological instability, *Nature*, *492: 243-247*.

Raterron, P., J. Girard, and J. H. Chen (2012), Activities of olivine slip systems in the upper mantle, *Physics of the Earth and Planetary Interiors*, *200*, 105-112.

Wang, D., Karato, S., and Li, Z-Y (2012), Influence of hydrogen on the electronic state of olivine: Implications for electrical conductivity *Geophys. Res. Lett.*, *39*.

Wang, D., Guo, Y., Yu, Y. and Karato, S. (2012), Electrical conductivity of amphibole-bearing rocks: Influence of dehydration., *Contrib. Mineral. Petrol.*, *164: 17-25*.

Wang, S., X Yu, J Zhang, M Chen, J Zhu, L Wang, D He, Z Lin, R Zhang, et. al. (2012), Experimental invalidation of phase-transition-induced elastic softening in CrN, , *Phys. Rev. B: Condens. Matter*, *86, 064111*

Yu, X., Jianzhong Zhang, Yingying Zhang, Liping Wang, and Yusheng Zhao (2012), Comparative Studies of Yield Strength and Elastic Compressibility Between Nanocrystalline and Bulk Cobalt, *J. Appl. Phys.*, *111, 113506*.

Yu, X., Raterron, P., Zhang, J., Lin, Z., Wang, L., Zhao, Y. (2012), Constitutive Law and Flow Mechanism in Diamond Deformation, *Scientific Reports*, *2, 876*.

2011

Akdogan, E., I Savkliyildiz, B Berke, Z Zhong, L Wang, M Vaughan, T Tsakalakos (2011), High Pressure Phase Transformation in MgO-Y2O3 Nanocomposites, *Appl. Phys. Lett.*, *99, 141915*

Dobson, D., S Hunt, A Lindsay-scott, I Wood (2011), Towards Better Analogues for MgSiO3 Post-Perovskite: NaCoF3 and NaNiF3, two new recoverable post-perovskite phases, *Phys. Earth Planet. Interiors*, *189, 171-175*

Hunt, S. A., A. M. Walker, R. J. McCormack, D. P. Dobson, A. Wills, and L. Li (2011), The effect of pressure on thermal diffusivity in pyroxenes, , *Mineralogical Magazine*, *75*(5), 2597–2610.

Karato, S. (2011), Some issues on the strength of the lithosphere, *Journal of Earth Science*, *22*, 131-136.

Karato, S. (2011), Rheological properties of the mantle of super-Earth：Some insights from mineral physics, *Icarus*, *212*, 14-23.

Karato, S. (2011), Water distribution across the mantle transition zone and its implications for global material circulation, *Earth and Planetary Science Letters*, *301*, 413-423.

Kung, J., I Jackson, R Liebermann (2011), High-temperature Elasticity of Polycrystalline Orthoenstatite (MgSiO3), *Am. Mineral.*, *96(4), 577-585*

Liebermann, R. (2011), Multi-anvil, High-Pressure Apparatus: A Half Century of Development and Progress, *High Pressure Res.*, *31(4), 493-532*

Liebermann, R. (2011), Bob-san and High Pressure Science and Technology in Japan: A 40+-Year History, *Rev. High Pressure Sci. Tech.*, *21, 115-126*.

Lin, Z., J Zhang, B Li, L Wang, H Mao, R Hemley, Y Zhao (2011), Superhard Diamond/tungsten Carbide Nanocomposites, *Appl. Phys. Lett.*, *98, 121914*

Liu, W., M Whitaker, Q Liu, L Wang, N Nishiyama, Y Wang, A Kubo, T Duffy, B Li, (2011), Thermal Equation of State of CaIrO3 Post-perovskite *Phys. Chem. Miner.*, *38(5),* , 407-417

Liu, W., Q Zeng, Q Jiang, L Wang, B Li (2011), Density and Elasticity of Zr46Cu37.6Ag8.4Al8 Bulk Metallic Glass at High Pressure, *Scripta Mater.*, *65, 497-500*.

Long, H., D. J. Weidner, Li Li, J. Chen, and L. Wang (2011), Deformation of Olivine at Subduction Zone Conditions Determined from In situ Measurements with Synchrotron Radiation, *Physics of the Earth and Planetary Interior*, *186(1-2)* 23-35.

Raterron, P., J. H. Chen, T. Geenen, and J. Girard (2011), Pressure effect on forsterite dislocation slip systems: Implications for upper-mantle LPO and low viscosity zone *Physics of the Earth and Planetary Interiors*, *188(1-2)*, 26-36.

Umemoto, K., and R. M. Wentzcovitch (2011), Two-stage dissociation in MgSiO3 post-perovskite, *Earth and Planetary Science Letters*, *311*(3-4), 225-229.

Yu, X., J Zhang, L Wang, Z Ding, C Jin, Y Zhao (2011), Comparative Studies of Constitutive Properties of nanocrystalline and Bulk Iron During Compressive Deformation, *Acta Mater*, *59(9),* , 3384-3389

Zhu, J., Hongwu Xu, Jianzhong Zhang, Changqing Jin, Liping Wang, and Yusheng Zhao (2011), Thermal equations of state and phase relation of PbTiO3: A high P-T synchrotron x-ray diffraction study, *Journal of Applied Physics*, *110, 084103*.

Apppendix V MAC beamline statistics

See Excel File: MAC2014Report.xls